Widespread introgression across a phylogeny of 155 *Drosophila* genomes

Anton Suvorov[1,*,$], Bernard Y. Kim[2], Jeremy Wang[1], Ellie E. Armstrong[2], David Peede[3], Emmanuel R. R. D'Agostino[3], Donald K. Price[4], Peter Wadell[5], Michael Lang[6], Virginie Courtier-Orgogozo[6], Jean R. David[7,8], Dmitri Petrov[2], Daniel R. Matute[3,†,&], Daniel R. Schrider[1,†,&], and Aaron A. Comeault[9,†,&,*]

1. Department of Genetics, University of North Carolina, Chapel Hill, North Carolina. USA
2. Department of Biology, Stanford University, Stanford, CA, USA
3. Department of Biology, University of North Carolina, Chapel Hill, North Carolina. USA
4. School of Life Sciences, University of Nevada, Las Vegas. USA
5. School of Fundamental Sciences, Massey University, Palmerston North. New Zealand
6. CNRS, Institut Jacques Monod, Université de Paris. France
7. Laboratoire Evolution, Génomes, Comportement, Ecologie (EGCE) CNRS, IRD, Univ. Paris-sud, Université Paris-Saclay, Gif sur Yvette, France
8. Institut de Systématique, Evolution, Biodiversité, CNRS, MNHN, UPMC, EPHE, Muséum National d'Histoire Naturelle, Sorbonne Universités, Paris, France
9. School of Natural Sciences, Bangor University, Bangor, Gwynedd, LL57 2DGA, UK

[$]Lead Contact
*Correspondence: antony.suvorov@med.unc.edu and a.comeault@bangor.ac.uk
[†]These authors contributed equally to this work.
[&]Senior authors

ABSTRACT

Genome-scale sequence data have invigorated the study of hybridization and introgression, particularly in animals. However, outside of a few notable cases, we lack systematic tests for introgression at a larger phylogenetic scale across entire clades. Here we leverage 155 genome assemblies, from 149 species, to generate a fossil-calibrated phylogeny and conduct multilocus tests for introgression across nine monophyletic radiations within the genus *Drosophila*. Using complementary phylogenomic approaches, we identify widespread introgression across the evolutionary history of *Drosophila*. Mapping gene-tree discordance onto the phylogeny revealed that both ancient and recent introgression has occurred across most of the nine clades that we examined. Our results provide the first evidence of introgression occurring across the evolutionary history of *Drosophila* and highlight the need to continue to study the evolutionary consequences of hybridization and introgression in this genus and across the Tree of Life.

INTRODUCTION

The extent of gene exchange in nature has remained one of the most hotly debated questions in speciation genetics. Genomic data have revealed that introgression is common across taxa, having been identified in major groups such as fungi[1–3], vertebrates[4–7], insects[8–10], and angiosperms[11,12]. The evolutionary effects of introgression are diverse, and are determined by multiple ecological and genomic factors[13,14]. Once thought to be strictly deleterious, it has become increasingly clear that introgression can serve as a source of genetic variation used during local adaptation[15,16] and adaptive radiation[17,18]. While our understanding of introgression as a widespread phenomenon has clearly improved, it remains unclear how often it occurs across taxa. Ideally, determining the frequency of introgression across the Tree of Life would leverage the signal from systematic analyses of clade-level genomic data without an *a priori* selection of taxa known to hybridize in nature.

At the phylogenetic scale, hybridization has typically been explored at relatively recent timescales. For example, studies of hybridization between cats (Felidae; 10-12 My; ~40 species[19]), butterflies (*Heliconius*; 10-15 My; 15 species[8]), cichlid fishes from the African rift lakes (0.5-10 My; ~27 species[18,20,21]), and wild tomatoes (*Solanum*; ~4 My; ~20 species[12]) all rejected a purely bifurcating phylogenetic history. In each of these systems introgression has occurred relatively recently, as the common ancestor for each species group occurred no more than 15 million years ago. However, there are also notable exceptions, and evidence for introgression has been found across much deeper phylogenetic timescales within vascular plants[11] and primates[7]. In some species, there is also evidence that introgression has been a source of adaptive genetic variation that has helped drive adaptation (e.g. refs. 2,22–25). These results show how introgression has both (1) occurred in disparate taxonomic groups and (2) promoted adaptation and diversification in some. Notwithstanding key examples[4–7,11,12], we still require systematic tests of introgression that use clade-level genomic data that spans both deep and shallow phylogenetic time to better understand introgression's generality throughout evolution.

Species from the genus *Drosophila* remain one of the most powerful genetic systems to study animal evolution. Comparative analyses suggest that introgression might be common during speciation in the genus[26]. Genome scans of closely related drosophilid species have provided evidence of gene flow and introgression[9,10,27–32]. There is also evidence of

contemporary hybridization[33–35] and stable hybrid zones between a handful of species[36–38]. These examples of hybridization and introgression show that species boundaries can be porous but cannot be taken as *prima facie* evidence of the commonality of introgression. We still lack a systematic understanding of the relative frequency of hybridization and subsequent introgression across *Drosophila*. Here we analyze patterns of introgression across a phylogeny generated using 155 whole genomes derived from 149 species of *Drosophila*, and the genomes of four outgroup species. These *Drosophila* species span over 50 million years of evolution and include multiple samples from nine major radiations within the genus *Drosophila*. We used two different phylogenetic approaches to test whether introgression has occurred in each of these nine radiations. We found numerous instances of introgression across the evolutionary history of drosophilid flies, some mapping to early divergences within clades up to 20-25 Mya. Our results provide a taxonomically unbiased estimate of the prevalence of introgression at a macroevolutionary scale. Despite few known observations of current hybridization in nature, introgression appears to be a widespread phenomenon across the phylogeny of *Drosophila*.

RESULTS

A high-confidence phylogeny of 155 *Drosophila* genomes

We first used genome-scale sequence data to infer phylogenetic relationships among species in our data set. To achieve this, we annotated and generated multiple sequence alignments for 2,791 Benchmarking Universal Single-Copy Orthologs (BUSCOs; v3[39,40]) across 155 independently assembled *Drosophila* genomes together with four outgroups (3 additional species from Drosophilidae and *Anopheles gambiae*). We used these alignments, totalling 8,187,056 nucleotide positions, and fossil calibrations to reconstruct a fossil-calibrated tree of *Drosophila* evolutionary history. Note that the inclusion of *Anopheles* as an outgroup allowed us to include a fossil of *Grauvogelia*, the oldest known dipteran, in our fossil calibration analysis, along with several *Drosophilidae* fossils and/or geological information (i.e., formation of the Hawaiian Islands; Data S1).

Our phylogenetic analyses (see Method Details for details) using both maximum-likelihood (ML using the `IQ-TREE` package) and gene tree coalescent-based (`ASTRAL`) approaches with DNA data revealed well-supported relationships among nearly all species within our dataset. Phylogenies inferred using these two approaches only differed in three

relationships (Figure S1): (i) *D. villosipedis* was either recovered as sister species to *D. limitata* + *D. ochracea* (ML topology) or as a sister to *D. limitata* + *D. ochracea* + *D. murphyi* + *D. sproati* (ASTRAL topology); (ii) *D. vulcana* and *D. seguyi* form monophyletic lineage sister to the *D. nikananu* + *D. spp. aff. chauvacae* + *D. burlai* + *D. bocqueti* + *D. bakoue* clade (ML topology) or have paraphyletic relationships where *D. vulcana* is sister to the *D. nikananu* + *D. spp. aff. chauvacae* + *D. burlai* + *D. bocqueti* + *D. bakoue* clade (ASTRAL topology) ; (iii) *D. simulans* was recovered as sister either to *D. mauritiana* (ML topology) or *D. sechellia* (ASTRAL topology, the latter of which is perhaps more likely to be the true species tree according to an analysis examining low-recombining regions, which are less prone to ILS[41]. The nodal supports were consistently high across both ML (Ultrafast bootstrap (UFBoot) = 100, an approximate likelihood ratio test with the nonparametric Shimodaira–Hasegawa correction (SH-aLRT) = 100, a Bayesian-like transformation of aLRT (aBayes) = 1) and ASTRAL (Local posterior probability (LPP) = 1) topologies with the exception of *D. limitata* + *D. ochracea* + *D. villosipedis* (UFBoot = 9, SH-aLRT = 81, aBayes = 1) and *D. carrolli* + *D. rhopaloa* + *D. kurseongensis* (UFBoot = 81.2, SH-aLRT = 81, aBayes = 1) on the ML tree, and *D. limitata* + *D. ochracea* + *D. murphyi* + *D. sproati* (LPP = 0.97) and *D. sulfugaster bilimbata* + *D. sulfugaster sulfurigaster* (LPP = 0.69) on the ASTRAL tree. Thus, the phylogeny we report here is the first of the genus *Drosophila* with almost all nodes resolved with high confidence—recent estimates of the *Drosophila* phylogeny lacked strong support throughout all tree depth levels[42–44].

Erroneous orthology inference as well as misalignment can impede accurate phylogenetic inference and create artificially long branches[45]. Repeating our ASTRAL analysis after removing outlier long branches via `TreeShrink`[45] resulted in an identical tree topology with the aforementioned ASTRAL tree (Figure S1). Furthermore, an ML topology estimated from the dataset with more closely related outgroup species (see Method Details) results in an identical topology with the aforementioned ML tree (Figure S1). The inferred phylogeny from the protein supermatrix showed only four incongruencies with the phylogeny that was inferred from DNA data (Figure S1): (i) *D. villosipedis* was recovered as a sister species to *D. limitata* + *D. ochracea* + *D. murphyi* + *D. sproati*; (ii) *D. watanabei* + *D. punjabiensis* is sister to the clade containing *D. bakoue* and *D. jambulina*; (iii) *D. vulcana* and *D. seguyi* show paraphyletic relationships; (iv) *Z. vittiger* and *Z. lachaisei* show sister species relationships. We performed further assessment of nodal support with Quartet Sampling[11], using the Quartet Concordance (QC) and Quartet

132 Differential (QD) scores to identify quartet-tree species-tree discordance (Method Details). At
133 some nodes, an appreciable fraction of quartets disagreed with our inferred species tree topology
134 (QC < 1), and in most of these cases this discordance was skewed toward one of the two possible
135 alternative topologies (i.e. QD < 1 but > 0) as is consistent with introgression. We formally
136 explore this pattern below.

137 In order to estimate divergence times across the *Drosophila* phylogeny, we developed
138 five calibration schemes (A, B, C, D and "Russo"; Data S1) used in `MCMCtree`[46] and one
139 scheme based on the Fossilized Birth-Death (FBD) process[47] used in `BEAST2`[48] (BEAST2 FBD;
140 Data S1). Overall, four of the five `MCMCtree` schemes yielded nearly identical age estimates
141 with narrow 95 % credible intervals (CI), whereas scheme "Russo" (a fossil calibration strategy
142 closely matching that from[43]) showed slightly older estimates (Figure S2) with notably wider
143 95% CIs. Throughout this manuscript we use the time estimates obtained with scheme A. This
144 calibration analysis estimated that extant members of the genus *Drosophila* branched off from
145 the other Drosophilidae (*Leucophenga*, *Scaptodrosophila* and *Chymomyza*) ~53 Mya (95% CI:
146 50 - 56.6 Mya) during the Eocene Epoch of the Paleogene Period (Figure 1). The same analysis
147 inferred that the split between the two major lineages within *Drosophila*—the subgenera of
148 *Sophophora* and *Drosophila*—occurred ~47 Mya (95% CI: 43.9- 49.9 Mya; Figure 1; "A" and
149 "B" clades, respectively); previously published estimates of this time include ~32 Mya (95% CI:
150 25–40 Mya[49]), ~63 Mya (95% CI: 39–87 Mya[50]), and ~56 Mya (95% CI not available[43]). We
151 also note that our divergence time estimates of the *Drosophila* subgenus (~34 Mya, 95% CI: 31.6
152 - 36.8 Mya; clades 6 through 9) are somewhat younger than ~40 Mya, a previous estimate
153 reported in[51], although the latter had fairly wide confidence intervals (95% CI: 33.4 - 47.6 Mya).
154 On the other hand, divergence time estimates produced by the FBD scheme in `BEAST2` tend to
155 be older especially for deeper nodes (Figure S2). Also, CIs estimated by `BEAST2` were wider
156 than those from `MCMCTREE`. This can be explained by the fewer assumptions about fossil
157 calibration placement and age prior specification for methods that rely on the FBD process.
158 Additionally, we note that not all parameters of the BEAST2 FBD calibration scheme converged
159 (i.e., effective sample size < 100) even after 6×10^8 MCMC generations. Thus, the lack of a
160 thorough fossil record within *Drosophila* makes it difficult to accurately and precisely estimate
161 divergence times, and point estimates of divergence times should be interpreted with caution.
162

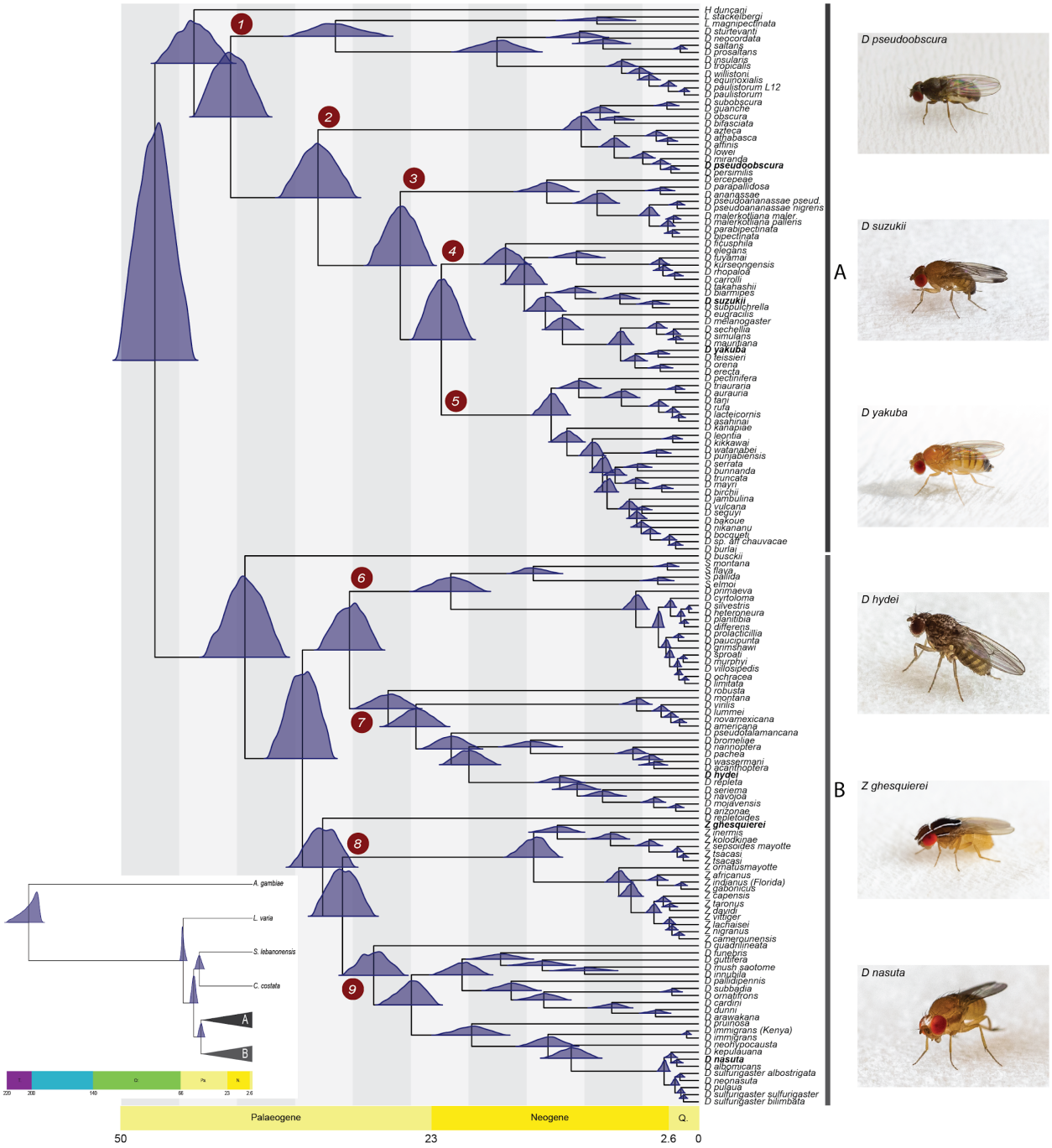

Fiure 1. Fossil calibrated maximum likelihood phylogenetic tree of the genus *Drosophila* inferred from a supermatrix of 2,791 BUSCO loci (total of 8,187,056 sites). The blue distributions at each divergence point on the tree represent nodal age posterior probabilities from MCMCTree. *Grauvogelia* and *Oligophryne* fossils were used to set priors on the age of the root of the tree, *Phytomyzites* and *Electrophortica succini* were used for priors for the root of the Drosophilidae family, and *Electrophortica succini* and *Scaptomyza dominicana* were used to set priors for the crown group "*Scaptomyza*", i.e. Most Recent Common Ancestor (MRCA) node of the *Scaptomyza* species (scheme A; Data S1). The numbered red circles denote clades for which analyses of introgression were performed. Inset: the phylogenetic and temporal relationships between our distant outgroup *Anopheles gambiae*, more closely

173 related outgroup species of Drosophilidae (*Leucophenga varia*, *Scaptodrosophila lebanonensis* and *Chymomyza*
174 *costata*), and the *Drosophila* genus. A and B denote the two inferred major groups within *Drosophila*.

175

176 **Widespread signatures of introgression across the *Drosophila* phylogeny**

177 To assess the prevalence of introgression across the *Drosophila* tree, we subdivided
178 species into nine monophyletic lineages (herein referred to as clades 1 through 9; Figure 1) and
179 tested for introgression within each clade. These clades correspond to the deepest divergences
180 within the genus, with most having an MRCA during the Paleogene. Clades 4 and 5 are the two
181 exceptions, splitting from an MRCA later in the Neogene. Within each of the nine clades, the
182 MRCA of all sampled genomes ranged from ~10 Mya (Figure 1; clade 2) to ~32 Mya (Figure 1;
183 clade 1). We note that *Hirtodrosophila duncani*, *Drosophila busckii* and *Drosophila repletoides*
184 were not included in these clade assignments as each of these species was the only sampled
185 descendent of a deep lineage; additional taxon sampling is required to assign them to specific
186 monophyletic species groups that could be tested for introgression.

187 We tested for introgression within each of these nine clades using two complementary
188 phylogenomic methods that rely on the counts of gene trees inferred from the BUSCO loci that
189 are discordant with the inferred trees (hereafter referred to as the discordant-count test or DCT)
190 and the distribution of branch lengths for discordant gene trees (hereafter termed the branch-
191 length test or BLT), respectively, among rooted triplets of taxa (Figure 2). These methods
192 leverage information contained across a set of gene trees to differentiate patterns of discordance
193 that are consistent with introgression from those that can be explained by incomplete lineage
194 sorting alone (see Method Details). We found at least one pair of species with evidence of
195 introgression in 7 of the 9 clades according to both DCT and BLT (i.e. the same pair of species
196 showed evidence for introgression that was significant for both tests in the same triplet at an
197 FDR-corrected *P*-value threshold of 0.05). In clades 1 and 3 there were no species pairs for
198 which the DCT and BLT were significant in the same triplet and both suggest the same
199 introgressing species pair (Data S2). However, both clades had several pairs that were significant
200 according to one test or the other (Data S2). We found even stronger support for introgression
201 using two existing software methods: QuIBL (Data S2), which examines the branch-length
202 distributions of all three gene tree topologies for a triplet[8], and HyDe (Data S2), which tests for
203 introgression by counting quartet site patterns[52]. Specifically, QuIBL detected introgression in
204 120 of 152 (78.9%) of species pairs detected by both DCT and BLT, as well as 894 additional

species pairs not detected by DCT-BLT; we note that BLT and QuIBL approaches are not fully independent, since they both utilize branch-length information. Similarly, HyDe detected introgression in 142 of 152 (93.4%) of species pairs detected by both DCT and BLT, and 898 additional species pairs (the results of HyDe were not qualitatively affected if a more distantly related outgroup, i.e. *Anopheles gambiae*, was selected, see Data S2). However, we focus here on the intersection between DCT and BLT methods (after correcting each for multiple testing), as this provides a more conservative estimate of the extent of introgression. Supporting this claim, we applied these tests to a gene tree dataset simulated under high levels of ILS[53] and observed low false positive rates: 0.054 for DCT, 0.089 for BLT, and 0.009 for their intersection.

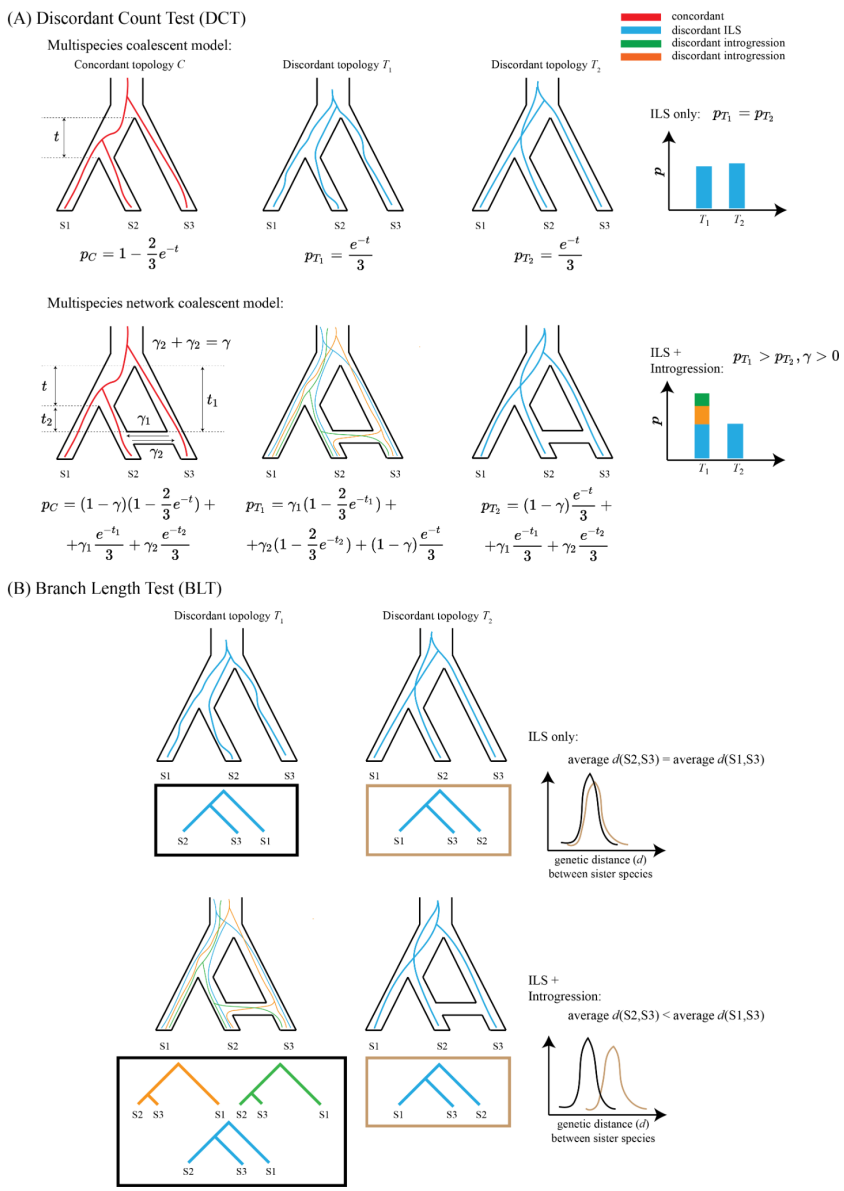

Figure 2. Overview of the phylogenomic approaches used to detect introgression. (A) The Discordant Count Test (DCT) identifies introgression where a given triplet within the tree shows an excess of gene trees that support one of the two possible divergent topologies. Note that concordant gene trees and corresponding probabilities are included for completeness, although these are not used by our test. (B) The Branch Length Test (BLT) identifies introgression where branch lengths of gene trees that support introgression are shorter than branch lengths of those that support the species tree and the less frequent divergent topology (i.e., the discordant topology putatively due to ILS).

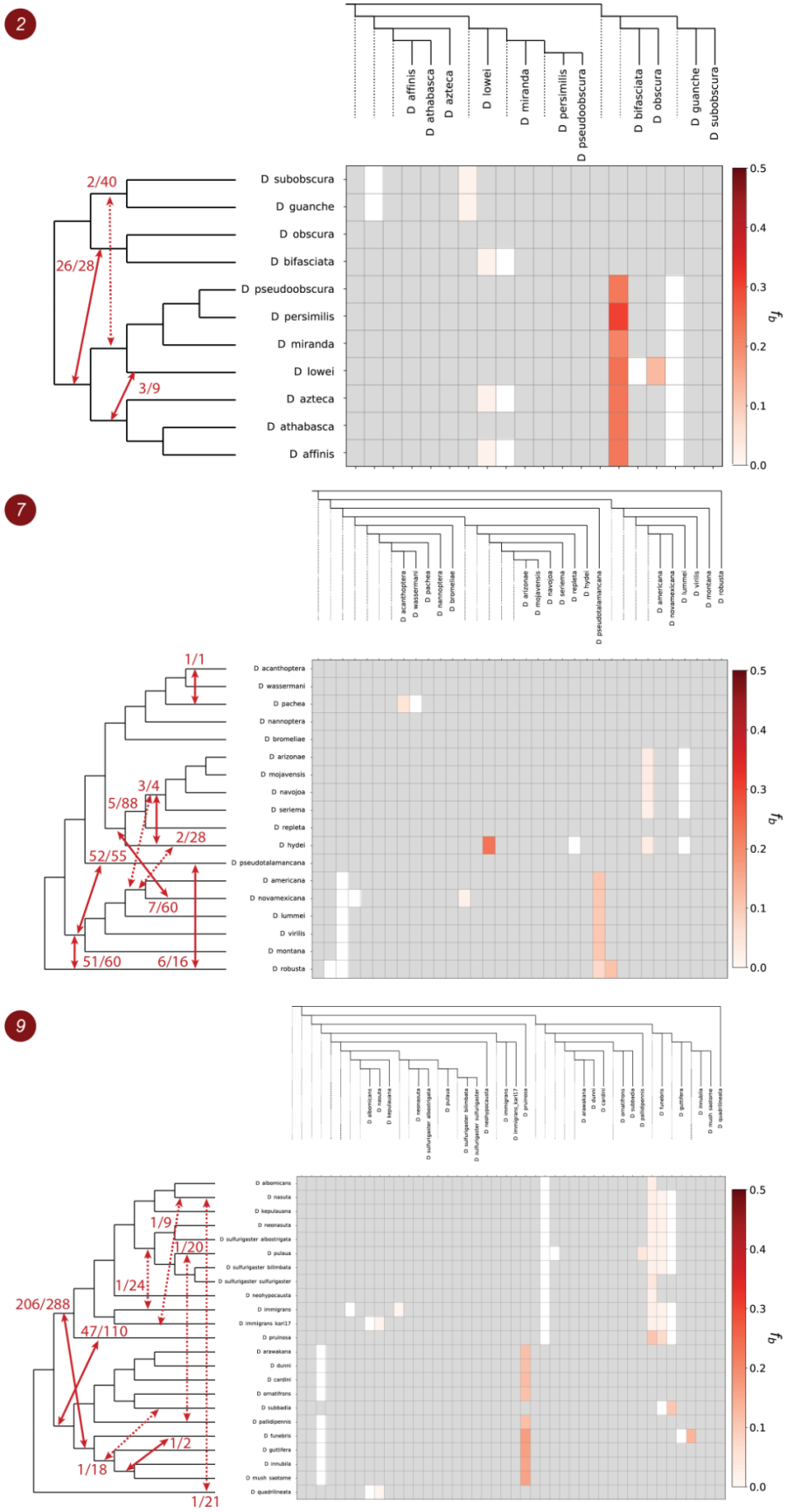
2
D affinis
D athabasca
D azteca
D lowei
D miranda
D persimilis
D pseudoobscura
D bifasciata
D obscura
D guanche
D subobscura
2/40
26/28
3/9
0.5
0.4
0.3
0.2
0.1
0.0
f_b
7
D acanthoptera
D wassermani
D pachea
D nannoptera
D bromeliae
D arizonae
D mojavensis
D navojoa
D seriema
D repleta
D hydei
D pseudotalamancana
D americana
D novamexicana
D lummei
D virilis
D montana
D robusta
1/1
3/4
5/88
2/28
52/55
7/60
51/60
6/16
9
D albomicans
D nasuta
D kepulauana
D neonasuta
D sulfurigaster albostrigata
D pulaua
D sulfurigaster bilimbata
D sulfurigaster sulfurigaster
D neohypocausta
D immigrans
D immigrans_kari17
D pruinosa
D arawakana
D dunni
D cardini
D ornatifrons
D subbadia
D pallidipennis
D funebris
D guttifera
D innubila
D mush saotome
D quadrilineata
1/9
1/20
1/24
206/288
47/110
1/2
1/18
1/21

236 **Figure 3.** Patterns of introgression inferred for the monophyletic clades 2, 7 and 9. The matrix shows inferred
237 introgression proportions as estimated from gene tree counts for the introgressed species pairs (Method Details), and
238 then mapped to internal branches using the *f*-branch method[20]. The expanded tree at the top of each matrix shows
239 both the terminal as well as ancestral branches. The tree on the left side of each matrix represents species
240 relationships with mapped introgression events (red arrows) derived from the corresponding *f*-branch matrix
241 (Method Details). The fractions next to each arrow represent the number of triplets that support a specific
242 introgression event by both DCT and BLT divided by the total number of triplets that could have detected the
243 introgression event. Dashed arrows represent introgression events with low support (triplet support ratio < 10%).
244
245
246 We carried out several analyses to assess the robustness of our results to data quality and
247 evolutionary rate. First, to assess the effect of alignment length we performed BLT and DCT
248 analyses on gene trees that excluded alignments with fewer than 1,000 sites. We found that ~
249 84% , ~94% and ~80% of introgressing species pairs that were identified by BLT, DCT, and
250 their intersection, respectively, remained significant after filtering out these short alignments
251 (Data S2). Second, we explored whether the rapid karyotype evolution[54] observed in the *obscura*
252 group (our clade 2) may impact introgression inference. To that end, we excluded loci that did
253 not belong to the same Muller element within each analyzed triplet by BLT and DCT. This
254 filtering scheme had a minor impact on introgression estimation with ~70% , ~89% and ~76%
255 introgressing taxon pairs identified by BLT, DCT and their intersection being identified after
256 filtering out loci that are found on different Muller elements in species within this clade (Data
257 S2). More importantly, this filtering had no impact on the introgression events discussed below
258 and shown in Figure 2—the exact same events were inferred for clade 2. Third, we investigated
259 the effects of evolutionary rate (as measured by d_N/d_S) heterogeneity across branches on
260 introgression inference. For each triplet tested by BLT and DCT we excluded gene trees with
261 $d_N/d_S > 0.53$, which corresponds to the 5% critical value of d_N/d_S distribution across all the
262 clades and gene trees. Overall, ~69%, ~82% and ~54% of our original number of introgressing
263 taxon pairs were identified after d_N/d_S filtering by the BLT, DCT and their intersection,
264 respectively (Data S2). Importantly, a large number of genes are removed when applying this
265 filter because only one branch within the portion of the gene tree relevant to the triplet must
266 exceed the critical value of d_N/d_S to result in the entire gene tree's removal. We therefore asked
267 to what extent this reduced fraction of introgressing taxon pairs is a consequence of reduced

power due to the reduction in the number of gene trees. We found that randomly subsampling gene trees without respect to d_N/d_S value can affect introgression inferences in a similar fashion: on average ~76% , ~85% and ~65% introgressing taxon pairs were identified by BLT, DCT and their intersection, respectively, after randomly removing the same number of genes removed by our d_N/d_S filter (see Method Details). Thus, although we don't rule out the possibility that evolutionary rate heterogeneity may influence our DCT-BLT analysis, or that the persistence of introgressed alleles may be correlated with a gene's evolutionary rate, this result shows that our estimates of gene flow are not being driven primarily by genes evolving under the least amount of selective constraint and/or the greatest amount of positive selection. We also repeated our BLT and DCT analyses using a gene tree set with potentially misaligned sequences removed via `TreeShrink` and obtained results largely concordant with other methods as shown in Data S2. However, we notice several exceptions: in clades 5 and 7 the number of species pairs with at least one triplet that is significant according to both the DCT and BLT methods is markedly higher after running `TreeShrink`, largely due to an increase in significant DCT results. In addition, for Hawaiian drosophilids (clade 6) we find no introgression based on the overlap between BLT and DCT.

The number of species pairs that show evidence of introgression in our initial DCT-BLT analysis is not equivalent to the number of independent introgression events among *Drosophila* species. This is because gene flow in the distant past can leave evidence of introgression in multiple contemporary species pairs. For example, we found evidence for introgression between *D. robusta* and all five species within the *D. americana-D. montana* group (see clade 7 in Figure 3). Rather than five independent instances of introgression between species, this pattern could reflect introgression between ancestral taxa that subsequently diverged into the contemporary species. More generally, cases where multiple introgressing species pairs each shared the same MRCA may be more parsimoniously explained by a single ancestral introgression event between the branches that coalesce at this node, while those involving only a single species pair may have resulted from introgression between the extant species pair (Data S2). Another example of the former can be seen in clade 6 where the evidence suggests introgression occurred between the Hawaiian *Scaptomyza* and *Drosophila* (Figure S3) that are estimated to have diverged from each other more than 20 Mya. This ancient introgression may have occurred prior to the formation of

298 Kauai island ~5 Mya which is now the oldest high island with extant species in these two
299 groups[55,56].
300 To summarize our DCT-BLT results and estimate both the number of introgression
301 events and the proportion of the genome that introgressed during those events (γ) we adapted the
302 *f*-branch heuristic[20] (implemented in `Dsuite`[57]; Method Details). Summed across all clades, our
303 *f*-branch results suggest that at least 30 introgression events are required to explain our DCT-
304 BLT results (Figure 3 and Figure S2). Clades 2, 4, 6, 7 and 9 showed the strongest evidence of
305 introgression, in terms of both the total number of DCT-BLT significant triplets and γ estimates
306 from `Dsuite` that support those events (Table 1). For example, in clade 2 Dsuite suggests an
307 ancestral introgression event between the branch leading to *D. obscura* and *D. bifasciata* and the
308 branch that leads to the clade containing *D. pseudoobscura* and *D. affinis*. Furthermore, this
309 particular signal is characterized by a large fraction of introgressed genetic material (γ = 0.237,
310 Table 1) and by the large number of triplets that are significant according to both DCT and BLT
311 (26 out of 28 total triplets that could detect this event are significant according to both tests). We
312 stress that both our methods used to detect introgression (DCT and BLT) and our approaches for
313 counting introgression events (*f*-branch) are conservative, and thus the true number of events
314 could be substantially greater, as suggested by our analyses using QuIBL and HyDe. Regardless
315 of the method used, careful examination of results in Data S2, Figure 3 and Figure S2 reveals
316 that deep introgression events are clearly the best explanation for some of our patterns (e.g. the
317 case from clade 7 involving *D. robusta* described above), although more recent events may have
318 occurred as well (e.g. between *D. pachea* and *D. acanthoptera*; Data S2, clade 7).
319 We note that some scenarios of ancestral population structure could potentially result in
320 differences in the number and branch lengths of gene trees with either discordant topology
321 (discussed in Method Details). We therefore applied a more stringent version of the DCT-BLT
322 that compares the branch lengths of the discordant topology with those of the concordant
323 topology; this test will not be sensitive to ancestral population structure but could potentially
324 produce many false negatives (Method Details). When applying this more stringent branch-
325 length test to our data set, we find that of the 511 triplets significant according to our combined
326 DCT-BLT test, 144 (28.1%) remain significant when imposing this much more stringent version
327 of the BLT (again, after FDR correction). We then asked how many of the 30 introgression
328 events shown in Figs. 3 and S3 were significant by this more stringent test for at least one triplet,

329 finding that 13 of the 30 events (43.3%) are significant, including 11/17 (64.7%) of the most
330 strongly supported events (those significant in at least 10% of triplets in our original analysis and
331 shown in solid lines in Figs. 3 and S3). This result shows that the majority (~2/3) of our strongly
332 supported putative introgression events are inconsistent with the phenomenon of ancestral
333 population structure-produced false positives. Given that this test is highly conservative, we
334 interpret this result as evidence that the vast majority of our detected introgression events are true
335 positives rather than artifacts of population structure.

336 To complement our *f*-branch analysis, we also used PhyloNet[58,59] to identify branches
337 with the strongest signature of introgression in each of the nine monophyletic clades in our tree.
338 Within each clade, we examined all possible network topologies produced by adding a single
339 reticulation event to the species tree and determined which of the resulting phylogenetic
340 networks produced the best likelihood score. We note that networks with more reticulation
341 events would most likely exhibit a better fit to observed patterns of introgression but the
342 biological interpretation of complex networks with multiple reticulations is more challenging;
343 thus, we limited the analysis to a single reticulation event even though this will produce false
344 negatives in clades with multiple gene flow events.

Clade	Introgression Event	Triplet ratio (significant/total)	Average γ	CI lower and upper bounds of lineage duration (Mya)
2	*D. obscura…D. bifasciata ↔ D. pseudoobscura…D. affinis*	26/28	0.237	9.84-5.9, 11.53-6.18
	D. subobscura…D. guanche ↔ D. pseudoobscura…D. lowei	2/40	0.016	9.84-1.93, 8.39-3.94
	D. lowei ↔ D. azteca…D. affinis	3/9	0.019	5.77-0, 8.39-2.88
4	*D. ficusphila ↔ D. carrolli…D. elegans*	5/81	0.049	18.46-0, 16.72-8.55
	D. ficusphila ↔ D. erecta…D. eugracilis	19/65	0.035	18.46-0, 14.77-10.3
	D. erecta...D. orena ↔ D. mauritiana...D. melanogaster	4/16	0.044	6.38-2.45, 7.71-2.92
5	*D. leontia ↔ D. birchii...D. serrata*	1/55	0.076	3.07-0, 8.84-6.4*

6	*S. pallida* ↔ *D. cyrtoloma...D. primaeva*	13/42	0.03	4.9-0, 24.22-4.52
	S. flava...S. montana ↔ *D. cyrtoloma...D. prolacticillia*	25/56	0.032	16.14-1.87/6.56-3.05
	D. primaeva ↔ *D. cyrtoloma...D. silvestris*	1/40	0.02	6.56-0/3.96-2
	D. heteroneura ↔ *D. grimshawi...D. sproati*	1/36	0.021	1.1-0/3.22-2.17*
	D. primaeva ↔ *D. prolacticillia*	1/12	0.012	6.56-0/2.16-0
7	*D. robusta* ↔ *D. americana...D. montana*	49/60	0.113	29.36-0/26.88-4.28
	D. pseudotalamancana ↔ *D. americana...D. montana*	52/55	0.103	23.56-0/26.88-4.28
	D. novamexicana ↔ *D. arizonae...D. hydei*	7/60	0.019	2.99-0/23.56-10.24
	D. americana...D. novamexicana ↔ *D. arizonae...D. seriema*	5/88	0.031	2.99-1.17/12.23-6.71*
	D. hydei ↔ *D. americana...D. novamexicana*	2/28	0.034	13.82-0/2.99-1.17
	D. hydei ↔ *D. arizonae...D. seriema*	3/4	0.234	13.82-0/12.23-6.71
	D. robusta ↔ *D. pseudotalamancana*	6/16	0.076	29.36-0/23.56-0
	D. pachea ↔ *D. acanthoptera*	1/1	0.05	5.36-0/4.95-0
8	*Z. camerounensis* ↔ *Z. lachaisei*	1/1	0.051	2.13-0/2.76-0
	Z. camerounensis ↔ *Z. vittiger*	1/2	0.06	2.13-0/3-0
9	*D. pruinosa* ↔ *D. arawakana...D. mush sãotomé*	47/110	0.138	22.41-0/27.26-18.21
	D. funebris...D. mush sãotomé ↔ *D. albomicans…D. pruinosa*	206/288	0.031	22.7-14.74/27.26-16.86
	D. subbadia ↔ *D. guttifera…D. mush sãotomé*	1/18	0.106	3.19-0/19.51-11.12*

D. innubila…D. mush sãotomé ↔ D. funebris	1/2	0.135	15.94-7.48/19.51-0
D. immigrans ↔ D. neonasuta...D. sulfurigaster sulfurigaster	1/24	0.01	1.44-0/3.5-1.7*
D. immigrans (kari17) ↔ D. nasuta	1/9	0.013	1.44-0/2.38-0
D. pallidipennis ↔ D. pulaua	1/20	0.045	18.35-0/1.86-0
D. quadrilineata ↔ D. nasuta	1/21	0.01	30.52-0/2.38-0

Table 1. Placements, support and timing of introgression events across the *Drosophila* phylogeny. Putative introgression events (↔) are specified between different clades indicated by the pair of species in that clade with the oldest MRCA. The triplet ratio shows the number of significant and non-significant triplets according to DCT-BLT. The average γ was obtained from the *f*-branch results. The durations of the two introgressing lineages are represented by predicted lower and upper boundaries of credible intervals (95% CIs) estimated by MCMCTree using calibration scheme A. * indicates introgressing lineages with no time overlap (according to 95% CIs).

For all clades except clade 8, the networks with the highest likelihood scores from PhyloNet qualitatively agree with the inferred introgression patterns by the DCT-BLT results summarized by `Dsuite`: the best-supported position of a reticulation event inferred by PhyloNet tended to occur in the same or similar locations on the tree as introgression events we inferred with our DCT-BLT analysis (Figure S4). On the other hand, PhyloNet inferred an introgression event in clade 8 that is more ancient than that inferred by DCT-BLT (an introgression event between *Z. capensis* and the *Z. camerounensis-Z. nigranus* ancestor detected by DCT-BLT is pushed back to the *Z. camerounensis-Z. vittiger* ancestor by `PhyloNet`). Uncertainty over the precise history of introgression in clade 8 notwithstanding, PhyloNet is consistent with our DCT-BCT analysis and identifies introgression across the *Drosophila* phylogeny.

Finally, we asked whether the proportion of the genome that introgressed between putatively introgressing taxa (γ) varied with the timing of introgression events (Figure 4). Rather than timing introgression relative to when two hybridizing taxa shared a most recent common ancestor (which would require additional data, such as haplotype lengths of introgressed regions), we leveraged divergence time estimates across the drosophila phylogeny (Figure 1) and

368 estimated when introgression events could have occured in time relative to the present (i.e.,
369 Mya). For this analysis, we focused on the 17 "best-supported" introgression events based on
370 the criteria that more than 10% of the total triplets that could detect introgression between a
371 given pair of taxa were significant according to both DCT and BLT (see solid red arrows in Figs.
372 3 and S3; Table 1). We estimated when these events occurred by taking the maximum,
373 minimum, and midpoint times when the two branches that experienced introgression both
374 coexisted in our dated phylogeny. We note that this approach results in imprecise time estimates,
375 particularly for long branches in the phylogeny; however, it allowed us to test whether there was
376 any obvious relationship between the proportion of the genome that introgressed (γ) and when
377 those introgression events took place in the past. In one instance, the two branches that putatively
378 experienced introgression did not overlap in time in our phylogeny. This situation could be
379 explained by "ghost" introgression with unsampled or extinct lineages. For the 17 remaining
380 introgression events, there was not a significant relationship between the midpoint estimate of
381 timing of introgression (Mya) and γ (Spearman's rank correlation: 0.43; $P = 0.085$; Figure 4).
382 Our analyses therefore support introgression across the evolutionary history of *Drosophila*, with
383 introgressing species pairs exchanging a similar fraction of the genome (range of average γ
384 estimates = 0.013 - 0.237) regardless of whether those events were ancient or more recent.
385

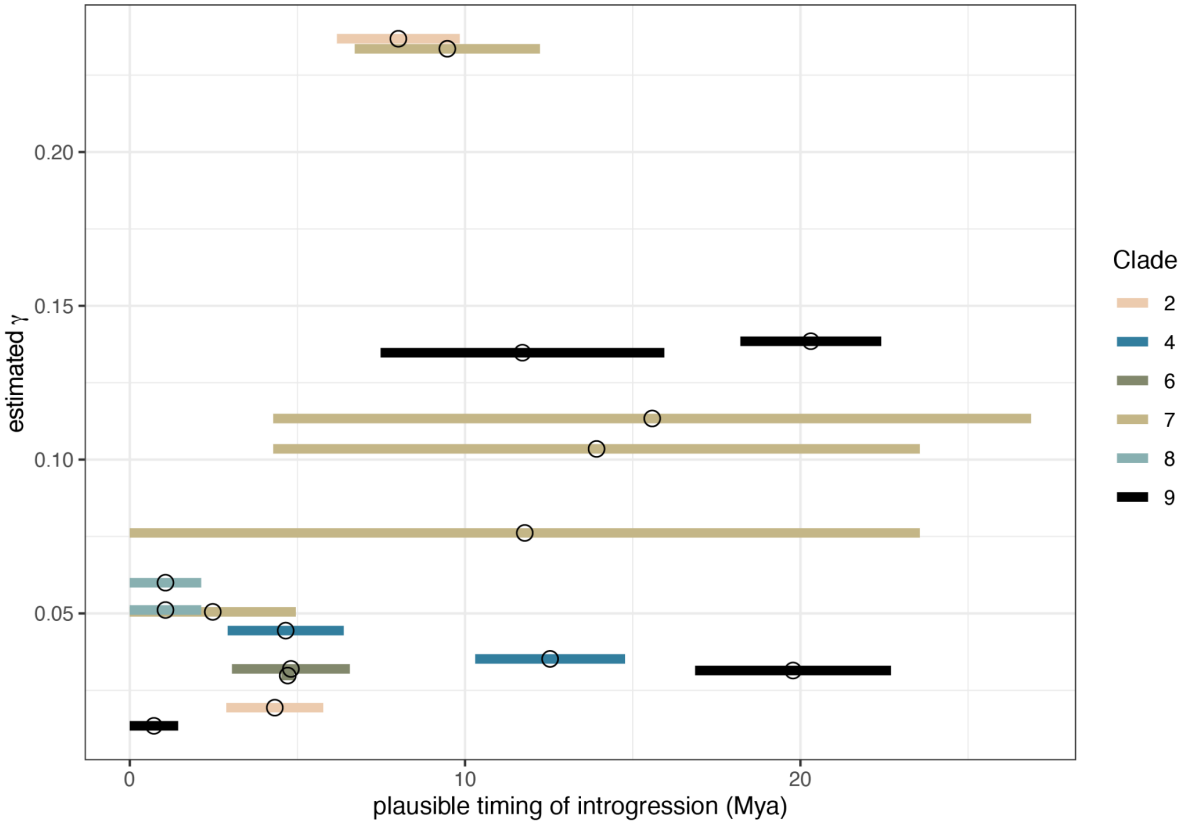

Figure 4. Time and fraction of the genome introgressing for the 17 best-supported introgression events across the *Drosophila* phylogeny. Each horizontal segment summarises one of the 17 introgression events highlighted in Figure 3 and is colored by clade. Segments span the times when the two putatively introgressing taxa both existed and are based on times inferred from the dating analysis summarised in Figure 1. Fraction of the genome that introgressed was estimated as the average f-branch statistic across all triplet comparisons that supported a given introgression event. Mya = million years ago.

Discussion

A time-calibrated tree of drosophilid evolution

Drosophila, as a genus, remains a premier model in genetics, ecology, and evolutionary biology. With over 1,600 species[42], the genus has the potential to reveal why some groups are more speciose than others. Yet the phylogenetic relationships among the main groups in the genus have remained largely unresolved (reviewed in [42]). Here we estimated a robust time-calibrated phylogeny for the whole genus using multilocus genomic data and calibrated it using a fossil record.

Our results confirm that the genus *Drosophila* is paraphyletic, with the genera *Zaprionus*, *Scaptomyza*, *Leucophenga*, and *Hirtodrosophila* each nested within the larger genus *Drosophila*.

404 Consistent with the subdivisions previously proposed by refs. 60 and 44, clades 1-5 of our
405 phylogeny contain species belonging to the subgenus *Sophophora*, and include species from the
406 genus *Lordiphosa* (group A in Figure 1). Clades 6-9 of our phylogeny contain species belonging
407 to the subgenus *Drosophila* (group B in Figure 1) and include species from the Hawaiian
408 *Drosophila* and the subgenera *Siphlodora*, *Phloridosa* (synonymized with the subgenus
409 *Drosophila*[44], and genus *Zaprionus*. For more recent radiations within *Drosophila*, the topology
410 we present is largely congruent with previous studies[42,51] but two general observations are
411 notable. First, our results confirm that *Lordiphosa* is closely related to the *saltans* and *willistoni*
412 groups (clade 1) and part of the *Sophophora* subgenus (consistent with ref. [61]). Second, we
413 confirm that *Zaprionus* is related to the *cardini/qunaria/immigrans* group (consistent with refs.
414 42 and 60, but discordant with 43). Despite our well resolved phylogeny, comparisons with other
415 studies emphasize the need to expand species sampling, especially given the potential to generate
416 highly contiguous genomes at relatively low cost[62].
417 Our results from divergence time analysis via `MCMCTree` suggest that the origin of
418 *Drosophila* (including the subgenera *Sophophora* (group A) and *Drosophila* (group B)) occurred
419 during the Eocene Epoch of the Paleogene, which is younger than estimates by [60] and [43], but
420 older than estimates by [49]. Different estimates of divergence times may be the result of different
421 calibration information used, such as mutation rates, the time of formation of the Hawaiian
422 Islands, and the fossil record. However, our comparison of various calibration schemes suggests
423 that the choice of calibration information has a minor effect on `MCMCTree`'s age estimation
424 (Figure S2). Additionally, credible intervals around our estimates tend to be notably narrower
425 than in all of the aforementioned studies. In contrast to the previous studies, we used genome-
426 scale multilocus data which would be expected to improve both the accuracy and precision of
427 age estimates[63,64].
428 On the other hand, we note that our analyses in `BEAST2` using the FBD model yielded
429 significantly older ages (Figure S2) especially for deeper nodes and with markedly wider
430 credible intervals suggesting origination of *Drosophila* lineage in the Late Cretaceous. These
431 calibration inconsistencies may arise as a result of the poor fossil record within *Drosophila* (only
432 *Scaptomyza dominicana* from Dominican amber) and selection of the oldest fossils for deeper
433 radiations, which together can lead to overestimation of nodal ages under the FBD model[65].

434 Moreover, the poor convergence behavior we observed would also be expected to produce larger
435 credible intervals.
436
437 **The extent of introgression in *Drosophila***
438 Access to genome-scale data has reinvigorated the study of hybridization and
439 introgression[14]. We used genome-scale sequence data to provide the first systematic survey of
440 introgression across the phylogeny of drosophilid flies. Our complementary—and
441 conservative—approaches identified overlapping evidence for introgression within seven of the
442 nine clades we analyzed (Figs. 3 and S3, Data S2). We conclude that at least 30 pairs of lineages
443 have experienced introgression across *Drosophila*'s history (Table 1), though we note that other
444 methods recover more introgression events (Data S2) and thus we cannot rule out the possibility
445 that the true number is substantially higher. Moreover, we find that in many cases a substantial
446 fraction of the genome is introgressed: our estimates indicate that numerous introgression events
447 have altered gene tree topologies for >10% of the genome (Figs. 3 and S3, Table 1). Studies in
448 contemporary *Drosophila* species suggest that selection may constrain the evolution of mixed
449 ancestry, at least in naturally occurring[9,36,66] and experimental admixed populations[67,68]. The
450 results we have presented here used phylogenetic signals to show that introgression has
451 nonetheless occurred and left a detectable signal within the genomes of many extant *Drosophila*.
452 In addition to providing an estimate of the extent of introgression, our results are
453 informative about the timing of introgression among *Drosophila* lineages: the approaches we
454 used to estimate the number of introgression events, and map them onto the phylogeny could
455 potentially overestimate the timing of introgression if multiple independent more recent events
456 are mistaken for one ancestral event. However, as described in the Results, both our PhyloNet
457 analyses and a careful examination of our DCT-BLT results are most consistent with ancient
458 introgression events in many cases. We also find evidence for very recent events, and although
459 our analyses did not search for gene flow between sister taxa, previous studies of closely related
460 species in *Drosophila* have revealed evidence of introgression[9,10,29,31,32]. Studies that have taken
461 phylogenomic approaches to detect introgression in other taxa have also reported evidence for
462 introgression between both "ancient" lineages (i.e., those that predate speciation events
463 generating extant species) and extant species[8,12,18,19,21]. We conclude that introgression between
464 *Drosophila* flies has similarly occurred throughout their evolutionary history.

465 Although the signal of introgression across our phylogeny provides evidence for
466 widespread introgression in *Drosophila*, the evolutionary role of introgressed alleles remains to
467 be tested. For example, the impact of hybridization and introgression on evolution can be
468 diverse, from redistributing adaptive genetic variation[23,69,70] to generating negative epistasis
469 between alleles that have evolved in different genomic backgrounds (refs. 71–73; reviewed in
470 refs. 15,16,74,75). The number of introgressed alleles that remain in a hybrid lineage depends on
471 their selection coefficients[76–78], their location in the genome (i.e., sex chromosomes vs.
472 autosomes[79–81]), levels of divergence between the hybridizing species[9,82,83], and recombination
473 rates among loci[6,84]. Previous studies have, for example, shown that *Drosophila* hybrids often
474 show maladaptive phenotypes[36,85–89]. Similarly, experimental hybrid swarms generated from two
475 independent species pairs of *Drosophila* have shown that these populations can evolve to
476 represent only one of their two parental species within as few as 10 generations, with the genome
477 of one of their two parental species being rapidly purged from the populations[67]. These results
478 show how hybrid *Drosophila* can be less fit than their parents, and further work is needed to
479 determine the evolutionary effects, and the ecological context, of the introgression that we report
480 here. However, our results suggest that not all introgressed material is deleterious in *Drosophila*,
481 as we find that for some lineages a large fraction of the genome is introgressed (i.e. our γ
482 estimates shown in Figs. 3 and S3 and Table 1). These results add to the growing body of
483 literature that document a detectable phylogenetic signal of introgession left within the genomes
484 of a wide range of species radiations that include *Drosophila*, other dipterans[90],
485 lepidopterans[8,84,91], humans[5,92,93], fungi[1,2], and angiosperm plants[11,12].
486
487 **Caveats and future directions**
488 We estimated the number of events required to explain the introgression patterns across
489 the tree and in some cases those events were recovered as relatively ancient. However, our
490 approaches for mapping gene flow events onto the phylogeny was somewhat parsimonious in
491 that it favors older events over repeated and recent introgressions (see Method Details), and thus
492 may bias the age of introgression towards ancient events and underestimate the true number of
493 pairs of lineages that have exchanged genetic material. For example, introgression events we
494 inferred at deeper nodes in our phylogeny are often supported by only a subset of comparisons
495 between species pairs that spanned those nodes (e.g. see "ancient" introgression events in clades

496 2, 7 and 9; Figure 3). It is also possible that some patterns we observe reflect scenarios where
497 introgressed segments have persisted along some lineages but been purged along others. This
498 phenomenon could also cause older gene flow between sister lineages, which should generally be
499 undetectable according to the BLT and DCT methods, to instead appear as introgression between
500 non-sister lineages that our methods can detect. Future work could seek to more precisely reveal
501 the number and timing of gene flow events across this phylogeny, including more recent
502 introgression events and gene flow between extant and extinct/unsampled lineages, a pattern
503 referred to as "ghost" introgression[94,95].
504 Our analyses also do not identify the precise alleles that have crossed species boundaries
505 or reveal the manner in which these alleles may have affected fitness in the recipient
506 population[74,75]. Genome alignments, complete annotations, and/or population level sampling
507 across the genus are required to determine whether certain genes or functional categories of
508 genes are more likely to cross species boundaries than others. More complete taxonomic
509 sampling, combined with methodological advances for inferring the number and timing of
510 introgression events in large phylogenies, will increase our ability to identify the specific timing
511 and consequences of introgression across *Drosophila*.
512
513 **Conclusions**
514 Speciation research has moved away from the debate of whether speciation can occur
515 with gene flow to more quantitative tests of how much introgression occurs in nature, and how
516 this introgression affects the fitness of individuals in the recipient population. Our well-resolved
517 phylogeny and survey of introgression revealed that gene flow has been a relatively common
518 feature across the evolutionary history of *Drosophila*. Yet, identifying the specific consequences
519 of introgression on fitness and the evolution of species and entire radiations within *Drosophila*
520 and other systems remains a major challenge. Future research could combine the power of
521 phylogenomic inference with population-level sampling to detect segregating introgression
522 between sister species to further our understanding of the amount, timing, and fitness
523 consequences of admixture for diversification.
524
525
526

527 **METHOD DETAILS**

528 **Genome assemblies and public data**

529 Genome sequences used by this work were obtained from concurrent projects and public
530 databases. Genome sequencing and assembly for 84 genomes is described in[62]. These data are
531 available for download at NCBI BioProject PRJNA675888. For the remaining genomes:
532 sequencing and assembly of 8 Hawaiian *Drosophila* were provided by E. Armstrong and D.
533 Price, described in Armstrong et al. (in prep) and available at NCBI BioProject PRJNA593822;
534 sequences and/or assemblies of five *nannoptera* group species were provided by M. Lang and V.
535 Courtier-Orgogozo and are available at NCBI BioProject PRJNA611543; 44 were downloaded
536 as assembled sequences from NCBI GenBank; *Z. sepsoides* and *D. neohypocausta* were
537 sequenced as paired-end 150bp reads on Illumina HiSeq 4000 at UNC and assembled using
538 SPAdes v3.11.1 with default parameters[103]; and 15 were generated by assembling short read
539 sequences downloaded from NCBI SRA. For sets of unassembled short reads, we used ABySS
540 v2.2.3[104] with parameters "k=64" with paired-end reads (typically 100-150bp) to assemble the
541 reads. Finally, outgroup genome sequences (*A. gambiae*, *M. domestica*, *L. trifolii*, *C. hians*, and
542 *E. gracilis*) were obtained from NCBI GenBank. See Data S3 for a full list of samples, strain
543 information, accessions, and associated publications.

544

545 **Orthology Inference**

546 We identified single-copy orthologous genes in each genome using BUSCO
547 (Benchmarking Universal Single-Copy Orthologs; v3.1.0[98]). BUSCO was run with orthologs
548 from the Diptera set in OrthoDB v.9 (odb9) using default parameters. For each species, all
549 BUSCOs found in a single copy were used for phylogenetic analysis.

550

551 **Assignment of BUSCO genes to Muller elements for *obscura* group species**

552 Each of the BUSCO genes identified as single-copy in each of the group 12 (*obscura*
553 group: *D. affinis*, *D. athabasca*, *D. azteca*, *D. bifasciata*, *D. guanche*, *D. lowei*, *D. miranda*, *D.*
554 *obscura*, *D. persimilis*, *D. pseudoobscura*, *D. subobscura*) genome assemblies was assigned to
555 one of the six Muller elements (elements A-F). For *D. athabasca*, *D. bifasciata*, *D. lowei*, *D.*
556 *miranda*, *D. pseudoobscura*, and *D. subobscura*, contig/scaffold associations with chromosomes
557 and/or Muller elements were simply obtained from NCBI GenBank assembly report tables. For

558 the remaining genomes (*D. affinis*, *D. azteca*, *D. guanche*, *D. obscura*, *D. persimilis*), we used
559 whole-genome alignments to infer the Muller element associated with each contig or scaffold.
560 Using the Progressive Cactus[105] software, each remaining genome was aligned to a closely
561 related reference genome (*D. affinis - D. athabasca; D. azteca - D. athabasca; D. guanche - D.*
562 *subobscura*; *D. obscura - D. bifasciata; D. persimilis - D. miranda*) with a similar
563 karyotype[54,106]. Using the reference genomes as backbones, each remaining genome was then
564 scaffolded, with Ragout[107]. The scaffolds allowed us to annotate each contig in the remaining
565 genomes with Muller element information from the reference genomes (see Data S4). BUSCO
566 genes on unplaced contigs were ignored.
567
568 **Phylogenetic reconstruction**
569 Every DNA BUSCO locus was aligned with MAFFT v7.427[100] using the L-INS-i
570 method. We removed sites that had fewer than three non-gap characters from the resulting
571 multiple sequence alignments (MSAs). These trimmed MSAs were concatenated to form a
572 supermatrix. To assess the quality of the assembled supermatrices we computed pairwise
573 completeness scores in AliStat[108] (Figure S5) . We inferred a maximum likelihood (ML)
574 phylogenetic tree from the supermatrix (a.k.a. concatenated alignment) using IQ-TREE v1.6.5[99],
575 and treated the supermatrix as a single partition. IQ-TREE was run under GTR+I+G substitution
576 model, as inference under any other substitution model will not necessarily lead to better
577 accuracy of tree topology estimation[109]. To estimate the support for each node in this tree, we
578 used three different reliability measures. We did 1,000 ultrafast bootstrap (UFBoot) replicates[110]
579 and additionally performed an approximate likelihood ratio test with the nonparametric
580 Shimodaira–Hasegawa correction (SH-aLRT) and a Bayesian-like transformation of aLRT[111].
581 We used the ML gene trees obtained by IQ-TREE with a GTR+I+G substitution model for tree
582 inference in ASTRAL[96]. For the estimated ASTRAL tree we calculated the support of each node
583 using local posterior probabilities (LPP)[96]. Also, we created a gene tree set by removing taxa
584 with outlier branch lengths that were potentially produced by misaligned regions and/or incorrect
585 orthology inference in TreeShrink[45] under default parameters. This analysis resulted in a small
586 fraction of branches removed from our gene tree set (<5.5%)
587 We did two additional analyses to verify the robustness of our topology inference. First,
588 we inferred an ML tree using WAG+I+G substitution model from the protein supermatrix

589 obtained from concatenation of protein BUSCO MSAs. MSAs based on amino acid sequences
590 have been shown to have superior accuracy to DNA MSAs for distantly related species[112].
591 Second, to verify that long branch attraction did not distort our tree topology, we inferred an ML
592 tree under a GTR+I+G substitution model using a different set of outgroup species from the
593 DNA supermatrix. Specifically, instead of distantly related *Anopheles gambiae*, we used *Musca*
594 *domestica, Liriomyza trifolii*, *Curricula hians* and *Ephydra gracilis* together as our outgroup
595 species.
596
597 **Phylogenetic Support Analysis via Quartet Sampling**
598 We used quartet sampling (QS) as an additional approach to estimate phylogenetic
599 support[11]. Briefly, QS provides three scores for internal nodes: (*i*) quartet concordance (QC),
600 which gives an estimate of how sampled quartet topologies agree with the putative species tree;
601 (*ii*) quartet differential (QD) which estimates frequency skewness of the discordant quartet
602 topologies, and can be indicative of introgression if a skewed frequency observed, and (*iii*)
603 quartet informativeness (QI) which quantifies how informative sampled quartets are by
604 comparing likelihood scores of alternative quartet topologies. Finally, QS provides a score for
605 terminal nodes, quartet fidelity (QF), which measures a taxon "rogueness". We did QS analysis
606 using the DNA BUSCO supermatrix described above, specifying an IQ-TREE engine for quartet
607 likelihood calculations with 100 replicates (i.e. number of quartet draws per focal branch).
608
609 **Fossil Dating**
610 *MCMCTREE*: We implemented the Bayesian algorithm of MCMCTree v4.9h[46] with
611 approximate likelihood computation to estimate divergence times within *Drosophila* using
612 several calibration schemes (Data S1). First, we estimated branch lengths by ML and then the
613 gradient and Hessian matrices around these ML estimates in MCMCTree using the DNA
614 supermatrix and species tree topology estimated by IQ-TREE. Because large amounts of
615 sequence data are not essential for accurate fossil calibration[113], we performed dating analysis
616 using a random sample of 1,000 MSA loci (out of 2,791) for the sake of computational
617 efficiency. Thus, for this analysis the supermatrix was generated by concatenating 1,000
618 randomly selected gene-specific MSAs. Using fewer loci (10 and 100) for fossil calibration did
619 not drastically affect nodal age estimation (Figure S1). We removed sites that had less than 80

620 non-gap characters from all these supermatrices. Second, we used the gradient and Hessian
621 matrix, which constructs an approximate likelihood function by Taylor expansion[114], to perform
622 fossil calibration in MCMC framework. For this step we specified a GTR+G substitution model
623 with four gamma categories; birth, death and sampling parameters of 1, 1 and 0.1, respectively.
624 To model rate variation we used an uncorrelated relaxed clock. To ensure convergence, the
625 analysis was run ten times independently for 8×10^6 generations (first 10^6 generations were
626 discarded as burn-in), logging every 1,000 generations. We used the R package MCMCtreeR[101]
627 to visualize the calibrated tree.
628 *BEAST 2*: Additionally we performed fossil calibration using the Fossilized Birth-Death
629 (FBD) process[47] as implemented in the Bayesian framework of BEAST 2.6.3[48]. For scalability
630 purposes, we randomly selected 1,000 loci and then partitioned them into 10 supermatrices each
631 consistent of 100 different MSAs. Each of these 10 datasets was treated as a single partition in
632 the downstream analyses. Additionally, we removed sites that had less than 128 non-gap
633 characters from all these supermatrices. To perform fossil calibration, we used a GTR+G model
634 with four gmamma categories, and an optimized relaxed clock[115] was used to model rate
635 variation. For the FBD prior we specified an initial origin value of 230 Mya (which corresponds
636 to the age of oldest known dipteran fossil *Grauvogelia*), and the tree likelihood was conditioned
637 on the proportion of species sampled at present ($\boldsymbol{\rho} = 0.1$). The remaining priors were set to their
638 defaults. In order to directly compare divergence time estimation between BEAST 2 and
639 MCMCTree, we used the same fixed IQ-TREE species tree topology with several exceptions.
640 First, we did not fix the phylogenetic positions of contemporary *Scaptomyza* species and fossil
641 taxon *Scaptomyza dominicana* within its monophyletic group. Second, we did not constrain
642 relationships of outgroup species *L. varia*, *C. costata*, *S. lebanonensis* including fossil taxon
643 *Electrophortica succini*. Two additional fossils, *Oligophryne* and *Phytomyzites*, were specified
644 for Drosophilidae stem. Furthermore, to accomodate uncertainty of fossil dates we incorporated
645 age ranges for several fossils (Data S1). For each of the 10 datasets we ran 2 independent
646 MCMC chains for 6×10^8 generations with sampling frequency of 10,000 for each model
647 parameter. Additionally, we performed sampling from the prior distribution only. Convergence
648 was assessed using ESS in Tracer[102]. Divergence times were generated by taking means of
649 posterior nodal ages discarding 25% of the sampled trees as burn-in in TreeAnnotator for each
650 dataset. To drastically improve computational efficiency of likelihood calculations in all BEAST

651 2 analyses we used the program in conjunction with BEAGLE library[97] that enables GPU
652 utilization.
653
654 **Inferring Introgression Across the Tree**
655 *Gene tree-based methods:* In order to detect patterns of introgression we used three
656 different methods that rely on the topologies of gene trees, and the distributions of their
657 corresponding branch lengths, for triplets of species. If the true species tree is ((A, B), C), these
658 tests are able to detect cases of introgression between A and C, or between B and C. These
659 include two of the methods that we devised for this study, and which use complementary pieces
660 of information—the counts of loci supporting either discordant topology, and the branch-length
661 distributions of gene trees supporting these topologies, respectively—to test an introgression-free
662 null model.
663 The first method we developed was the discordant-count test (DCT), which compares the
664 number of genes supporting each of the two possible discordant gene trees: ((A, C), B) or (A, (B,
665 C)), similar in principle to the delta statistic from[116]. Genes may support the two discordant
666 topologies (denoted T_1 and T_2) in the presence of ILS and/or in the presence of introgression. In
667 the absence of ancestral population structure, gene genealogies from loci experiencing ILS will
668 show either topology with equal probability; ILS alone is not expected to bias the count towards
669 one of the topologies. In the presence of introgression, one of the two topologies will be more
670 frequent than the other because the pair of species experiencing gene flow will be sister lineages
671 at all introgressed loci (illustrated in Figure 2). For example, if there is introgression between A
672 and C, there will be an excess of gene trees with the ((A, C), B) topology. The DCT identifies
673 pairs of species that may have experienced introgression by performing a χ^2 goodness-of-fit test
674 on the gene tree count values for a species triplet to determine whether their proportions
675 significantly deviate from 0.5, the expected proportion for each gene genealogy under ILS. We
676 used this test on all triplets extracted from BUSCO gene trees within each clade, and the
677 resulting *P*-values were then corrected for multiple testing using the Benjamini-Hochberg
678 procedure with a false discovery rate (FDR) cutoff of 0.05. We note that these tests are not
679 independent since different triplets may contain overlapping taxa. Thus, while our correction
680 results in more conservative tests[57], the inferred FDRs may be somewhat inaccurate.

681 Second, we devised a branch-length test (BLT) to identify cases of introgression
682 (illustrated in Figure 2). This test examines branch lengths to estimate the age of the most recent
683 coalescence event (measured in substitutions per site). Introgression should result in more recent
684 coalescences than expected under the concordant topology with complete lineage sorting, while
685 ILS shows older coalescence events[90]. Importantly, ILS alone is not expected to result in
686 different coalescence times between the two discordant topologies, and this forms the null
687 hypothesis for the BLT. For a given triplet, for each gene tree we calculated the distance d (a
688 proxy for the divergence time between sister taxa) by averaging the external branch lengths
689 leading to the two sister taxa under that gene tree topology. We calculated d for each gene tree
690 and denote values of d from the first discordant topology d_{T1} and those from the second
691 discordant topology d_{T2}. We then compared the distributions of d_{T1} and d_{T2} using a Mann-
692 Whitney U test. Under ILS alone the expectation is that $d_{T1} = d_{T2}$, while in the presence of
693 introgression $d_{T1} < d_{T2}$ (suggesting introgression consistent with discordant topology T_1) or $d_{T1} >$
694 d_{T2} (suggesting introgression with consistent with topology discordant T_2). The BLT is
695 conceptually similar to the D3 test[117], which transforms the values of d_{T1} and d_{T2} in a manner
696 similar to the D statistic for detecting introgression[92]. As with the DCT, we performed the BLT
697 on all triplets within a clade and used a Benjamini-Hochberg correction with a false discovery
698 rate cutoff (FDR) of 0.05. We note that both the DCT and BLT will be conservative in cases
699 where, for a triplet ((A,B), C), there is introgression between A and C as well as B and C, with
700 the extreme case of equal rates of introgression for both species pairs resulting in a complete loss
701 of power.
702 Finally, we used QuIBL[8], an analysis of branch-length distribution across gene trees to
703 infer putative introgression patterns. Briefly, under coalescent theory internal branches of rooted
704 gene trees for a set of 3 taxa (triplet) can be viewed as a mixture of two distributions: one that
705 generates branch lengths under ILS, and the other under introgression/speciation. Thus, the
706 estimated mixing proportions (π_1 for ILS and π_2 for introgression/speciation; $\pi_1 + \pi_2 = 1$) of those
707 distribution components show which fraction of the gene trees were generated through ILS or
708 non-ILS processes. For a given triplet, QuIBL computes the proportion of gene trees that support
709 the three alternative topologies. Then for every alternative topology QuIBL estimates mixing
710 proportions along with other relevant parameters via Expectation-Maximization and computes
711 Bayesian Information Criterion (BIC) scores for ILS-only and introgression models. For

712 concordant topologies elevated values of π_2 are expected whereas for discordant ones π_2 values
713 significantly greater than zero are indicative of introgression. To identify significant cases of
714 introgression here we used a cutoff of ΔBIC < -30 as in[8]. We ran QuIBL on every triplet
715 individually under default parameters with the number of steps (the `numsteps` parameter) set
716 to 50 and using *Anopheles gambiae* for triplet rooting; the branch length between *A. gambiae* and
717 the triplet is not used for any of QuIBL's calculations.

718 We note that the DCT and BLT methods are potentially impacted by ancestral population
719 structure: if the lineages leading to B and C were in subpopulations that were more likely to
720 interbreed in the ancestral population, then the ((B, C), A) topology might be expected to be
721 more prevalent than ((A, C), B), along with a shorter time back to the first coalescence.
722 However, it is unclear how much of a concern ancestral population structure should be for this
723 analysis, as it seems less likely that it would be a pair of lineages that diverged first (i.e. A and C
724 or B and C) that interbred more frequently in the ancestral population instead of the two lineages
725 that went on to be sister taxa (i.e. A and B). Nonetheless, plausible scenarios of ancestral
726 structure supporting one discordant topology over the other can be devised (e.g. ref [118]). We
727 therefore conducted a more stringent version of our DCT-BLT combined test that requires the
728 average distance between the two introgressing taxa (when examining gene trees with the
729 discordant topology consistent with introgression) to be less than that between the two sister
730 species (when examining gene trees with the concordant topology). Such a pattern is consistent
731 with introgression between non-sister species, which must occur more recently than the species
732 split and therefore causing more recent coalescence events, but not with ancestral structure which
733 will still result in older coalescence times for discordant trees than the concordant trees (because
734 structure in the ancestral population is only a factor in the case of ILS). Note that this test is
735 expected to be especially conservative because ILS, which for many triplets accounts for a
736 sizable fraction of our discordant gene trees, will push the coalescent times for all discordant
737 topologies back further in time.

738 We also examined the effect of evolutionary rate heterogeneity measured in branch-
739 specific d_N/d_S values on introgression detection. To that end, we generated codon alignments for
740 each BUSCO locus using TranslatorX[119] and then calculated d_N/d_S ratios for each gene tree in
741 PAML[46] within each clade using a free-ratios branch model that assumes independent d_N/d_S for
742 each gene tree branch. Then, we evaluated the distribution of d_N/d_S ratios across all gene trees to

743 determine the 95th percentile value of d_N/d_S. Thus, we repeated our DCT/BLT analyses for each
744 triplet after excluding every gene tree that had at least one branch with $d_N/d_S > 0.53$. Note,
745 branches with d_N/d_S values where $d_S < 0.001$ or >5 were deemed unreliable and thus were
746 excluded from calculation of a critical value or from downstream filtering. Additionally, we
747 performed random filtering of gene trees to see if this procedure would have a similar impact on
748 downstream introgression-detection as did our d_N/d_S filter. First, we estimated the distribution of
749 proportions of gene trees retained for each triplet after applying the d_N/d_S filter. Then, for a
750 given triplet, we randomly drew a number of genes to remove from the aforementioned
751 distribution, and then applied our DCT-BLT method to this triplet after removing the selected
752 number of genes. This process was repeated for each triplet tested in our main analysis to
753 generate a randomly filtered set of DCT-BLT results for each of our 9 clades. We then repeated
754 this entire process 1000 times and noted the average fraction of DCT-BLT results remaining
755 significant after randomly filtering genes.
756 Our DCT-BLT test assumes that there is no recombination within loci and complete
757 inter-locus independence—these assumptions are commonly made by introgression inference
758 methods[10,120,121]. We note that intra-locus recombination may interfere with the signatures of
759 introgression by reducing discordant topology counts (because even loci experiencing
760 introgression will have non-introgressed segments), and similarly diluting branch-length
761 signatures of introgression, thereby reducing the sensitivity of our DCT-BLT approach.
762 Nevertheless, site-pattern-based approaches (e.g. HyDe, see below) are not affected by intra-
763 locus recombination as they evaluate each site in an MSA independently.
764
765 *Site-pattern -based detection of introgression*: Signatures of introgression can be identified by
766 investigating fractions of certain site patterns within MSAs of species quartets. One of the most
767 widely used methods is based on the counts of ABBA-BABA site patterns (aka., Patterson's D
768 statistic[122]). Here we used the hybridization model implemented in HyDe[52] that implements an
769 alternative invariant-based statistic to test introgression and estimate the fraction of the
770 introgressed genome (γ). We ran HyDe analysis on each of the 9 clades using the entire
771 supermatrix and in each case selected the quartet's outgroup from a sister clade. Additionally, to
772 examine effects of outgroup choice, we ran HyDe analyses with a more distantly related
773 outgroup, *Anopheles gambiae* for all clades. The resulting *P*-values for each quartet were

774 corrected for multiple testing using the Bonferroni method. To investigate an individual
775 contribution of each BUSCO locus to introgression, we additionally ran HyDe using BUSCO
776 MSAs with *Anopheles gambiae* outgroup. We note, however, in this case HyDe's power to
777 detect introgression will be reduced, especially for short MSAs with <10,000 sites[52]. A complete
778 summary for each BUSCO locus including introgression results from locus-specific HyDe and
779 BLT/DCT analyses is included in Data S5.
780
781 *Placing introgression events on the phylogeny*: All the aforementioned methods can infer
782 multiple correlated signatures of introgression especially when triplets/quartets share the same
783 taxa. Thus it can be difficult to interpret these interdependent results. To alleviate this problem,[20]
784 devised a simple heuristic metric called *f*-branch to disentangle and map introgression events
785 detected in multiple correlated species pairs onto the tree. In the original formulation, *f*-branch
786 examines multiple f_4 statistics measured for each species pair and that quantify γ, the proportion
787 of introgressed material for that pair. However, the calculation of the f_4 statistic requires allele
788 frequency measures within each sampled species. Thus, to calculate *f*-branch statistic, instead of
789 f_4 we used the introgression proportion derived from DCT/BLT as follows: $\gamma = \frac{dis_2 - dis_1}{con + dis_1 + dis_2}$,
790 where *con*, dis_1 and dis_2 represent concordant and discordant counts of gene trees and $dis_1 < dis_2$.
791 To compute *f*-branch statistic from DCT/BLT's γ estimates and to visualize the results within
792 each clade we used the `Dsuite` python package[57].
793 `Dsuite` outputs a matrix of γ estimates that have been partially collapsed: on one axis of
794 this matrix signals of introgression can appear on ancestral branches, but on the other axis only
795 extant branches are shown. Thus, we manually further collapsed these signatures by
796 parsimoniously assuming that if some lineage A showed evidence of introgression with multiple
797 descendants of some other lineage B that is not ancestral to A, then we considered this to be
798 caused by a single introgression event between A and B. Note that we did not require all
799 descendants of lineage B to share this signature of introgression, and thus this approach could
800 potentially undercount the number of introgression events and overestimate their ages.
801
802 *Phylogenetic networks:* Introgression generates instances of reticulate evolution such that purely
803 bifurcating trees cannot adequately represent evolutionary history; phylogenetic networks have
804 been shown to provide a better fit to describe these patterns[123,124]. We used PhyloNet[58,59] to

805 calculate likelihood scores for networks generated by placing a single reticulation event (node) in
806 an exhaustive manner, i.e. connecting all possible branch pairs within a clade. Because full
807 likelihood calculations with PhyloNet can be prohibitively slow for large networks, for each of
808 clades 1 through 9 we selected a subsample of 10 species in a manner that preserves the overall
809 species tree topology. No subsampling was performed for clade 3 which has fewer than 10
810 species. Using these subsampled clade topologies, we formed all possible network topologies
811 having a single reticulation node (with the exception of networks having reticulation nodes
812 connecting sister taxa). Because PhyloNet takes gene trees as input, for each clade we
813 subsampled each gene tree to include only the subset of 10 species selected for the PhyloNet
814 analysis (or all species in the case of clade 3); any gene trees missing at least one of these species
815 were omitted from the analysis. Finally, we used the GalGTProb program[125] of the PhyloNet
816 suite to obtain a likelihood score for each network topology for each clade. We report networks
817 with the highest likelihood scores.
818
819 **Data and code availability**
820 The data and code produced during this study are publically available on GitHub
821 (https://github.com/SchriderLab/drosophila_phylogeny) and FigShare
822 (dx.doi.org/10.6084/m9.figshare.13264697). Whole genome sequencing data generated for this
823 study are available on NCBI (BioProject PRJNA675888, BioProject PRJNA593822, and
824 BioProject PRJNA611543).
825
826 **Acknowledgements:** We thank M. Hahn, M. Turelli, A. Yassin, and M. Matschiner for helpful
827 feedback on a previous draft, and M. Hibbins for sharing simulated gene trees. AS and DRS
828 were supported by the NIH under award nos. R00HG008696 and R35GM138286. BYK was
829 supported by the NIH under award no. F32GM135998. JW was supported by the NIH under
830 award no. K01DK119582. DP, AAC were supported by NSF Dimensions of Biodiversity award
831 1737752. DRM and ERRD were supported by NIH award R01GM121750. The funders had no
832 role in study design, data collection and analysis, decision to publish, or preparation of the
833 manuscript.

834 **Competing interests:** The authors declare that there is no conflict of interest

References:

1. Tusso, S., Nieuwenhuis, B.P.S., Sedlazeck, F.J., Davey, J.W., Jeffares, D.C., and Wolf, J.B.W. (2019). Ancestral Admixture Is the Main Determinant of Global Biodiversity in Fission Yeast. Mol. Biol. Evol. *36*, 1975–1989.
2. Eberlein, C., Hénault, M., Fijarczyk, A., Charron, G., Bouvier, M., Kohn, L.M., Anderson, J.B., and Landry, C.R. (2019). Hybridization is a recurrent evolutionary stimulus in wild yeast speciation. Nat. Commun. *10*, 923.
3. Leducq, J.-B., Nielly-Thibault, L., Charron, G., Eberlein, C., Verta, J.-P., Samani, P., Sylvester, K., Hittinger, C.T., Bell, G., and Landry, C.R. (2016). Speciation driven by hybridization and chromosomal plasticity in a wild yeast. Nat. Microbiol. *1*, 15003.
4. Lamichhaney, S., Berglund, J., Almén, M.S., Maqbool, K., Grabherr, M., Martinez-Barrio, A., Promerová, M., Rubin, C.-J., Wang, C., Zamani, N., et al. (2015). Evolution of Darwin's finches and their beaks revealed by genome sequencing. Nature *518*, 371.
5. Racimo, F., Sankararaman, S., Nielsen, R., and Huerta-Sánchez, E. (2015). Evidence for archaic adaptive introgression in humans. Nat. Rev. Genet. *16*, 359–371.
6. Schumer, M., Xu, C., Powell, D.L., Durvasula, A., Skov, L., Holland, C., Blazier, J.C., Sankararaman, S., Andolfatto, P., Rosenthal, G.G., et al. (2018). Natural selection interacts with recombination to shape the evolution of hybrid genomes. Science *360*, 656–660.
7. Vanderpool, D., Minh, B.Q., Lanfear, R., Hughes, D., Murali, S., Harris, R.A., Raveendran, M., Muzny, D.M., Hibbins, M.S., Williamson, R.J., et al. (2020). Primate phylogenomics uncovers multiple rapid radiations and ancient interspecific introgression. PLOS Biol. *18*, e3000954.
8. Edelman, N.B., Frandsen, P.B., Miyagi, M., Clavijo, B., Davey, J., Dikow, R.B., García-Accinelli, G., Belleghem, S.M.V., Patterson, N., Neafsey, D.E., et al. (2019). Genomic architecture and introgression shape a butterfly radiation. Science *366*, 594–599.
9. Turissini, D.A., and Matute, D.R. (2017). Fine scale mapping of genomic introgressions within the Drosophila yakuba clade. PLOS Genet. *13*, e1006971.
10. Lohse, K., Clarke, M., Ritchie, M.G., and Etges, W.J. (2015). Genome-wide tests for introgression between cactophilic \textlessi\textgreaterDrosophila\textless/i\textgreater implicate a role of inversions during speciation. Evolution *69*, 1178–1190.
11. Pease, J.B., Brown, J.W., Walker, J.F., Hinchliff, C.E., and Smith, S.A. (2018). Quartet Sampling distinguishes lack of support from conflicting support in the green plant tree of life. Am. J. Bot. *105*, 385–403.
12. Pease, J.B., Haak, D.C., Hahn, M.W., and Moyle, L.C. (2016). Phylogenomics reveals three sources of adaptive variation during a rapid radiation. PLOS Biol. *14*, e1002379.
13. Rhymer, J.M., and Simberloff, D. (1996). Extinction by Hybridization and Introgression. Annu. Rev. Ecol. Syst. *27*, 83–109.
14. Taylor, S.A., and Larson, E.L. (2019). Insights from genomes into the evolutionary importance and prevalence of hybridization in nature. Nat. Ecol. Evol. *3*, 170–177.
15. Hedrick, P.W. (2013). Adaptive introgression in animals: examples and comparison to new mutation and standing variation as sources of adaptive variation. Mol. Ecol. *22*, 4606–4618.
16. Suarez-Gonzalez, A., Lexer, C., and Cronk, Q.C.B. (2018). Adaptive introgression: a plant perspective. Biol. Lett. *14*, 20170688.
17. Marques, D.A., Meier, J.I., and Seehausen, O. (2019). A Combinatorial View on Speciation and Adaptive Radiation. Trends Ecol. Evol. *34*, 531–544.

880 18. Meier, J.I., Marques, D.A., Mwaiko, S., Wagner, C.E., Excoffier, L., and Seehausen, O.
881 (2017). Ancient hybridization fuels rapid cichlid fish adaptive radiations. Nat. Commun. *8*,
882 14363.
883 19. Li, G., Davis, B.W., Eizirik, E., and Murphy, W.J. (2016). Phylogenomic evidence for
884 ancient hybridization in the genomes of living cats (Felidae). Genome Res. *26*, 1–11.
885 20. Malinsky, M., Svardal, H., Tyers, A.M., Miska, E.A., Genner, M.J., Turner, G.F., and
886 Durbin, R. (2018). Whole-genome sequences of Malawi cichlids reveal multiple radiations
887 interconnected by gene flow. Nat. Ecol. Evol. *2*, 1940–1955.
888 21. Svardal, H., Quah, F.X., Malinsky, M., Ngatunga, B.P., Miska, E.A., Salzburger, W.,
889 Genner, M.J., Turner, G.F., and Durbin, R. (2020). Ancestral Hybridization Facilitated
890 Species Diversification in the Lake Malawi Cichlid Fish Adaptive Radiation. Mol. Biol.
891 Evol. *37*, 1100–1113.
892 22. Chen, N., Cai, Y., Chen, Q., Li, R., Wang, K., Huang, Y., Hu, S., Huang, S., Zhang, H.,
893 Zheng, Z., et al. (2018). Whole-genome resequencing reveals world-wide ancestry and
894 adaptive introgression events of domesticated cattle in East Asia. Nat. Commun. *9*, 2337.
895 23. Jones, M.R., Mills, L.S., Alves, P.C., Callahan, C.M., Alves, J.M., Lafferty, D.J.R., Jiggins,
896 F.M., Jensen, J.D., Melo-Ferreira, J., and Good, J.M. (2018). Adaptive introgression
897 underlies polymorphic seasonal camouflage in snowshoe hares. Science *360*, 1355–1358.
898 24. Platt, R.N., McDew-White, M., Le Clec'h, W., Chevalier, F.D., Allan, F., Emery, A.M.,
899 Garba, A., Hamidou, A.A., Ame, S.M., Webster, J.P., et al. (2019). Ancient Hybridization
900 and Adaptive Introgression of an Invadolysin Gene in Schistosome Parasites. Mol. Biol.
901 Evol. *36*, 2127–2142.
902 25. Richards, E.J., and Martin, C.H. (2017). Adaptive introgression from distant Caribbean
903 islands contributed to the diversification of a microendemic adaptive radiation of trophic
904 specialist pupfishes. PLOS Genet. *13*, e1006919.
905 26. Turelli, M., Lipkowitz, J.R., and Brandvain, Y. (2014). On the Coyne and Orr-Igin of
906 Species: Effects of Intrinsic Postzygotic Isolation, Ecological Differentiation, X
907 Chromosome Size, and Sympatry on Drosophila Speciation. Evolution *68*, 1176–1187.
908 27. Brand, C.L., Kingan, S.B., Wu, L., and Garrigan, D. (2013). A Selective Sweep across
909 Species Boundaries in Drosophila. Mol. Biol. Evol. *30*, 2177–2186.
910 28. Dyer, K.A., Bewick, E.R., White, B.E., Bray, M.J., and Humphreys, D.P. (2018). Fine-scale
911 geographic patterns of gene flow and reproductive character displacement in Drosophila
912 subquinaria and Drosophila recens. Mol. Ecol. *27*, 3655–3670.
913 29. Garrigan, D., Kingan, S.B., Geneva, A.J., Andolfatto, P., Clark, A.G., Thornton, K.R., and
914 Presgraves, D.C. (2012). Genome sequencing reveals complex speciation in the Drosophila
915 simulans clade. Genome Res. *22*, 1499–511.
916 30. Kang, L., Garner, H.R., Price, D.K., and Michalak, P. (2017). A Test for Gene Flow among
917 Sympatric and Allopatric Hawaiian Picture-Winged Drosophila. J. Mol. Evol. *84*, 259–266.
918 31. Mai, D., Nalley, M.J., and Bachtrog, D. (2020). Patterns of Genomic Differentiation in the
919 Drosophila nasuta Species Complex. Mol. Biol. Evol. *37*, 208–220.
920 32. Schrider, D.R., Ayroles, J., Matute, D.R., and Kern, A.D. (2018). Supervised machine
921 learning reveals introgressed loci in the genomes of Drosophila simulans and D. sechellia.
922 PLOS Genet. *14*, e1007341.
923 33. Kao, J.Y., Lymer, S., Hwang, S.H., Sung, A., and Nuzhdin, S.V. (2015). Postmating
924 reproductive barriers contribute to the incipient sexual isolation of the United States and
925 Caribbean Drosophila melanogaster. Ecol. Evol. *5*, 3171–3182.

926 34. Matute, D.R., and Ayroles, J.F. (2014). Hybridization occurs between Drosophila simulans
927 and D. sechellia in the Seychelles archipelago. J. Evol. Biol. *27*, 1057–68.
928 35. Sawamura, K., Sato, H., Lee, C.-Y., Kamimura, Y., and Matsuda, M. (2016). A Natural
929 Population Derived from Species Hybridization in the Drosophila ananassae Species
930 Complex on Penang Island, Malaysia. Zoolog. Sci. *33*, 467–475.
931 36. Cooper, B.S., Sedghifar, A., Nash, W.T., Comeault, A.A., and Matute, D.R. (2018). A
932 Maladaptive Combination of Traits Contributes to the Maintenance of a Drosophila Hybrid
933 Zone. Curr. Biol. *28*, 2940-2947.e6.
934 37. Lachaise, D., Harry, M., Solignac, M., Lemeunier, F., Bénassi, V., and Cariou, M.L.
935 (2000). Evolutionary novelties in islands: *Drosophila santomea*, a new melanogaster sister
936 species from São Tomé. Proc. R. Soc. Lond. B *267*, 1487–1495.
937 38. Matute, D.R. (2010). Reinforcement of gametic isolation in *Drosophila*. PLoS Biol. *8*,
938 e1000341.
939 39. Seppey, M., Manni, M., and Zdobnov, E.M. (2019). BUSCO: Assessing Genome Assembly
940 and Annotation Completeness. In Gene Prediction: Methods and Protocols Methods in
941 Molecular Biology., M. Kollmar, ed. (Springer), pp. 227–245.
942 40. Waterhouse, R.M., Seppey, M., Simão, F.A., Manni, M., Ioannidis, P., Klioutchnikov, G.,
943 Kriventseva, E.V., and Zdobnov, E.M. (2017). BUSCO applications from quality
944 assessments to gene prediction and phylogenomics. Mol. Biol. Evol.
945 41. Pease, J.B., and Hahn, M.W. (2013). More Accurate Phylogenies Inferred from Low-
946 Recombination Regions in the Presence of Incomplete Lineage Sorting. Evolution *67*,
947 2376–2384.
948 42. O'Grady, P.M., and DeSalle, R. (2018). Phylogeny of the Genus Drosophila. Genetics *209*,
949 1–25.
950 43. Russo, C.A.M., Mello, B., Frazão, A., and Voloch, C.M. (2013). Phylogenetic analysis and
951 a time tree for a large drosophilid data set (Diptera: Drosophilidae). Zool. J. Linn. Soc. *169*,
952 765–775.
953 44. Yassin, A. (2013). Phylogenetic classification of the Drosophilidae Rondani (Diptera): the
954 role of morphology in the postgenomic era. Syst. Entomol. *38*, 349–364.
955 45. Mai, U., and Mirarab, S. (2018). TreeShrink: fast and accurate detection of outlier long
956 branches in collections of phylogenetic trees. BMC Genomics *19*, 272.
957 46. Yang, Z. (2007). PAML 4: Phylogenetic analysis by maximum likelihood. Mol. Biol. Evol.
958 *24*, 1586–1591.
959 47. Heath, T.A., Huelsenbeck, J.P., and Stadler, T. (2014). The fossilized birth–death process
960 for coherent calibration of divergence-time estimates. Proc. Natl. Acad. Sci. *111*, E2957–
961 E2966.
962 48. Bouckaert, R., Vaughan, T.G., Barido-Sottani, J., Duchêne, S., Fourment, M.,
963 Gavryushkina, A., Heled, J., Jones, G., Kühnert, D., Maio, N.D., et al. (2019). BEAST 2.5:
964 An advanced software platform for Bayesian evolutionary analysis. PLOS Comput. Biol.
965 *15*, e1006650.
966 49. Obbard, D.J., Maclennan, J., Kim, K.-W., Rambaut, A., O'Grady, P.M., and Jiggins, F.M.
967 (2012). Estimating Divergence Dates and Substitution Rates in the Drosophila Phylogeny.
968 Mol. Biol. Evol. *29*, 3459–3473.
969 50. Tamura, K., Subramanian, S., and Kumar, S. (2004). Temporal Patterns of Fruit Fly
970 (Drosophila) Evolution Revealed by Mutation Clocks. Mol. Biol. Evol. *21*, 36–44.
971 51. Izumitani, H.F., Kusaka, Y., Koshikawa, S., Toda, M.J., and Katoh, T. (2016).

Phylogeography of the Subgenus Drosophila (Diptera: Drosophilidae): Evolutionary History of Faunal Divergence between the Old and the New Worlds. PLOS ONE *11*, e0160051.

52. Blischak, P.D., Chifman, J., Wolfe, A.D., and Kubatko, L.S. (2018). HyDe: A Python Package for Genome-Scale Hybridization Detection. Syst. Biol. *67*, 821–829.
53. Hibbins, M., and Hahn, M. (2021). Phylogenomic approaches to detecting and characterizing introgression.
54. Bracewell, R., Chatla, K., Nalley, M.J., and Bachtrog, D. (2019). Dynamic turnover of centromeres drives karyotype evolution in Drosophila. eLife *8*, e49002.
55. Magnacca, K.N., and Price, D.K. (2015). Rapid adaptive radiation and host plant conservation in the Hawaiian picture wing Drosophila (Diptera: Drosophilidae). Mol. Phylogenet. Evol. *92*, 226–242.
56. Price, J.P., and Clague, D.A. (2002). How old is the Hawaiian biota? Geology and phylogeny suggest recent divergence. Proc. R. Soc. B Biol. Sci. *269*, 2429–2435.
57. Malinsky, M., Matschiner, M., and Svardal, H. (2021). Dsuite - Fast D-statistics and related admixture evidence from VCF files. Mol. Ecol. Resour. *21*, 584–595.
58. Than, C., Ruths, D., and Nakhleh, L. (2008). PhyloNet: a software package for analyzing and reconstructing reticulate evolutionary relationships. BMC Bioinformatics *9*, 322.
59. Wen, D., Yu, Y., Zhu, J., and Nakhleh, L. (2018). Inferring Phylogenetic Networks Using PhyloNet. Syst. Biol. *67*, 735–740.
60. Throckmorton, L.H. (1975). The phylogeny, ecolopy, and geography of *Drosophila*. In Handbook of Genetics, Vol 3., R. C. King, ed. (Plenum Publishing Corp.), pp. 421–469.
61. Katoh, T., Tamura, K., and Aotsuka, T. (2000). Phylogenetic Position of the Subgenus Lordiphosa of the Genus Drosophila (Diptera: Drosophilidae) Inferred from Alcohol Dehydrogenase (Adh) Gene Sequences. J. Mol. Evol. *51*, 122–130.
62. Kim, B.Y., Wang, J.R., Miller, D.E., Barmina, O., Delaney, E., Thompson, A., Comeault, A.A., Peede, D., D'Agostino, E.R.R., Pelaez, J., et al. (2020). Highly contiguous assemblies of 101 drosophilid genomes. bioRxiv, 2020.12.14.422775.
63. Reis, M.D., and Yang, Z. (2013). The unbearable uncertainty of Bayesian divergence time estimation. J. Syst. Evol. *51*, 30–43.
64. Yang, Z., and Rannala, B. (2006). Bayesian Estimation of Species Divergence Times Under a Molecular Clock Using Multiple Fossil Calibrations with Soft Bounds. Mol. Biol. Evol. *23*, 212–226.
65. Matschiner, M. (2019). Selective Sampling of Species and Fossils Influences Age Estimates Under the Fossilized Birth–Death Model. Front. Genet. *0*.
66. Meiklejohn, C.D., Landeen, E.L., Gordon, K.E., Rzatkiewicz, T., Kingan, S.B., Geneva, A.J., Vedanayagam, J.P., Muirhead, C.A., Garrigan, D., Stern, D.L., et al. (2018). Gene flow mediates the role of sex chromosome meiotic drive during complex speciation. eLife *7*, e35468.
67. Matute, D.R., Comeault, A.A., Earley, E., Serrato-Capuchina, A., Peede, D., Monroy-Eklund, A., Huang, W., Jones, C.D., Mackay, T.F.C., and Coyne, J.A. (2020). Rapid and Predictable Evolution of Admixed Populations Between Two Drosophila Species Pairs. Genetics *214*, 211–230.
68. Wang, S., Nalley, M.J., Chatla, K., Aldaimalani, R., MacPherson, A., Wei, K., Corbett, R., Mai, D., and Bachtrog, D. (2021). Neo-sex chromosome evolution shapes sex-dependent asymmetrical introgression barrier (Evolutionary Biology).

1018 69. Anderson, T.M., vonHoldt, B.M., Candille, S.I., Musiani, M., Greco, C., Stahler, D.R.,
1019 Smith, D.W., Padhukasahasram, B., Randi, E., Leonard, J.A., et al. (2009). Molecular and
1020 evolutionary history of melanism in North American gray wolves. Science *323*, 1339–1343.
1021 70. Dasmahapatra, K.K. (2012). Heliconius genome supplementary information. Nature.
1022 71. Fishman, L., and Sweigart, A.L. (2018). When Two Rights Make a Wrong: The
1023 Evolutionary Genetics of Plant Hybrid Incompatibilities. Annu. Rev. Plant Biol. *69*, 707–
1024 731.
1025 72. Maheshwari, S., and Barbash, D.A. (2011). The Genetics of Hybrid Incompatibilities.
1026 Annu. Rev. Genet. *45*, 331–355.
1027 73. Nosil, P., and Schluter, D. (2011). The genes underlying the process of speciation. Trends
1028 Ecol. Evol. *26*, 160–167.
1029 74. Baack, E.J., and Rieseberg, L.H. (2007). A genomic view of introgression and hybrid
1030 speciation. Curr. Opin. Genet. Dev. *17*, 513–518.
1031 75. Moran, B.M., Payne, C., Langdon, Q., Powell, D.L., Brandvain, Y., and Schumer, M.
1032 (2020). The genetic consequences of hybridization. ArXiv201204077 Q-Bio.
1033 76. Harris, K., and Nielsen, R. (2016). The Genetic Cost of Neanderthal Introgression. Genetics
1034 *203*, 881–891.
1035 77. Kim, B.Y., Huber, C.D., and Lohmueller, K.E. (2018). Deleterious variation shapes the
1036 genomic landscape of introgression. PLOS Genet. *14*, e1007741.
1037 78. Sachdeva, H., and Barton, N.H. (2018). Introgression of a Block of Genome Under
1038 Infinitesimal Selection. Genetics *209*, 1279–1303.
1039 79. Geraldes, A., Ferrand, N., and Nachman, M.W. (2006). Contrasting Patterns of
1040 Introgression at X-Linked Loci Across the Hybrid Zone Between Subspecies of the
1041 European Rabbit (Oryctolagus cuniculus). Genetics *173*, 919–933.
1042 80. Payseur, B.A., Krenz, J.G., and Nachman, M.W. (2004). Differential Patterns of
1043 Introgression Across the X Chromosome in a Hybrid Zone Between Two Species of House
1044 Mice. Evolution *58*, 2064–2078.
1045 81. Storchová, R., Reif, J., and Nachman, M.W. (2010). Female Heterogamety and Speciation:
1046 Reduced Introgression of the Z Chromosome Between Two Species of Nightingales.
1047 Evolution *64*, 456–471.
1048 82. Hamlin, J.A.P., Hibbins, M.S., and Moyle, L.C. (2020). Assessing biological factors
1049 affecting postspeciation introgression. Evol. Lett. *4*, 137–154.
1050 83. Kronforst, M.R., Hansen, M.E.B., Crawford, N.G., Gallant, J.R., Zhang, W., Kulathinal,
1051 R.J., Kapan, D.D., and Mullen, S.P. (2013). Hybridization Reveals the Evolving Genomic
1052 Architecture of Speciation. Cell Rep., 666–677.
1053 84. Martin, S.H., Davey, J.W., Salazar, C., and Jiggins, C.D. (2019). Recombination rate
1054 variation shapes barriers to introgression across butterfly genomes. PLOS Biol. *17*,
1055 e2006288.
1056 85. Coyne, J.A., and Orr, H.A. (1997). "Patterns of speciation in *Drosophila*" revisited.
1057 Evolution *51*, 295–303.
1058 86. Coyne, J.A., and Orr, H.A. (1989). Patterns of speciation in *Drosophila*. Evolution *43*, 362–
1059 381.
1060 87. Serrato-Capuchina, A., Schwochert, T.D., Zhang, S., Roy, B., Peede, D., Koppelman, C.,
1061 and Matute, D.R. (2020). Pure species discriminate against hybrids in the Drosophila
1062 melanogaster species subgroup. bioRxiv, 2020.07.22.214924.
1063 88. Turissini, D.A., McGirr, J.A., Patel, S.S., David, J.R., and Matute, D.R. (2018). The Rate of

1064 Evolution of Postmating-Prezygotic Reproductive Isolation in Drosophila. Mol. Biol. Evol.
1065 *35*, 312–334.
1066 89. Turissini, D.A., Comeault, A.A., Liu, G., Lee, Y.C.G., and Matute, D.R. (2017). The ability
1067 of *Drosophila* hybrids to locate food declines with parental divergence. Evolution *71*, 960–
1068 973.
1069 90. Fontaine, M.C., Pease, J.B., Steele, A., Waterhouse, R.M., Neafsey, D.E., Sharakhov, I.V.,
1070 Jiang, X., Hall, A.B., Catteruccia, F., Kakani, E., et al. (2015). Extensive introgression in a
1071 malaria vector species complex revealed by phylogenomics. Science *347*.
1072 91. Dasmahapatra, K.K., Walters, J.R., Briscoe, A.D., Davey, J.W., Whibley, A., Nadeau, N.J.,
1073 Zimin, A.V., Hughes, D.S.T., Ferguson, L.C., Martin, S.H., et al. (2012). Butterfly genome
1074 reveals promiscuous exchange of mimicry adaptations among species. Nature *487*, 94–98.
1075 92. Green, R.E., Krause, J., Briggs, A.W., Maricic, T., Stenzel, U., Kircher, M., Patterson, N.,
1076 Li, H., Zhai, W., Fritz, M.H.-Y., et al. (2010). A Draft Sequence of the Neandertal Genome.
1077 Science *328*, 710–722.
1078 93. Juric, I., Aeschbacher, S., and Coop, G. (2015). The Strength of Selection Against
1079 Neanderthal Introgression. PLoS Genet. *12*, e1006340.
1080 94. Durvasula, A., and Sankararaman, S. (2020). Recovering signals of ghost archaic
1081 introgression in African populations. Sci. Adv. *6*, eaax5097.
1082 95. Ottenburghs, J. (2020). Ghost Introgression: Spooky Gene Flow in the Distant Past.
1083 BioEssays *42*, 2000012.
1084 96. Sayyari, E., and Mirarab, S. (2016). Fast Coalescent-Based Computation of Local Branch
1085 Support from Quartet Frequencies. Mol. Biol. Evol. *33*, 1654–1668.
1086 97. Ayres, D.L., Darling, A., Zwickl, D.J., Beerli, P., Holder, M.T., Lewis, P.O., Huelsenbeck,
1087 J.P., Ronquist, F., Swofford, D.L., Cummings, M.P., et al. (2012). BEAGLE: An
1088 Application Programming Interface and High-Performance Computing Library for
1089 Statistical Phylogenetics. Syst. Biol. *61*, 170–173.
1090 98. Simão, F.A., Waterhouse, R.M., Ioannidis, P., Kriventseva, E.V., and Zdobnov, E.M.
1091 (2015). BUSCO: assessing genome assembly and annotation completeness with single-copy
1092 orthologs. Bioinformatics *31*, 3210–3212.
1093 99. Nguyen, L.-T., Schmidt, H.A., von Haeseler, A., and Minh, B.Q. (2015). IQ-TREE: A Fast
1094 and Effective Stochastic Algorithm for Estimating Maximum-Likelihood Phylogenies. Mol.
1095 Biol. Evol. *32*, 268–274.
1096 100. Katoh, K., Misawa, K., Kuma, K., and Miyata, T. (2002). MAFFT: a novel method for
1097 rapid multiple sequence alignment based on fast Fourier transform. Nucleic Acids Res. *30*,
1098 3059–3066.
1099 101. Puttick, M.N. (2019). MCMCtreeR: functions to prepare MCMCtree analyses and visualize
1100 posterior ages on trees. Bioinformatics *35*, 5321–5322.
1101 102. Rambaut, A., Drummond, A.J., Xie, D., Baele, G., and Suchard, M.A. (2018). Posterior
1102 Summarization in Bayesian Phylogenetics Using Tracer 1.7. Syst. Biol. *67*, 901–904.
1103 103. Bankevich, A., Nurk, S., Antipov, D., Gurevich, A.A., Dvorkin, M., Kulikov, A.S., Lesin,
1104 V.M., Nikolenko, S.I., Pham, S., Prjibelski, A.D., et al. (2012). SPAdes: A New Genome
1105 Assembly Algorithm and Its Applications to Single-Cell Sequencing. J. Comput. Biol. *19*,
1106 455–477.
1107 104. Jackman, S.D., Vandervalk, B.P., Mohamadi, H., Chu, J., Yeo, S., Hammond, S.A., Jahesh,
1108 G., Khan, H., Coombe, L., Warren, R.L., et al. (2017). ABySS 2.0: resource-efficient
1109 assembly of large genomes using a Bloom filter. Genome Res. *27*, 768–777.

1110 105. Armstrong, J., Hickey, G., Diekhans, M., Fiddes, I.T., Novak, A.M., Deran, A., Fang, Q.,
1111 Xie, D., Feng, S., Stiller, J., et al. (2020). Progressive Cactus is a multiple-genome aligner
1112 for the thousand-genome era. Nature *587*, 246–251.
1113 106. Bracewell, R., and Bachtrog, D. (2020). Complex Evolutionary History of the Y
1114 Chromosome in Flies of the Drosophila obscura Species Group. Genome Biol. Evol. *12*,
1115 494–505.
1116 107. Kolmogorov, M., Armstrong, J., Raney, B.J., Streeter, I., Dunn, M., Yang, F., Odom, D.,
1117 Flicek, P., Keane, T.M., Thybert, D., et al. (2018). Chromosome assembly of large and
1118 complex genomes using multiple references. Genome Res. *28*, 1720–1732.
1119 108. Wong, T.K.F., Kalyaanamoorthy, S., Meusemann, K., Yeates, D.K., Misof, B., and Jermiin,
1120 L.S. (2020). A minimum reporting standard for multiple sequence alignments. NAR
1121 Genomics Bioinforma. *2*.
1122 109. Abadi, S., Azouri, D., Pupko, T., and Mayrose, I. (2019). Model selection may not be a
1123 mandatory step for phylogeny reconstruction. Nat. Commun. *10*, 934.
1124 110. Minh, B.Q., Nguyen, M.A.T., and von Haeseler, A. (2013). Ultrafast approximation for
1125 phylogenetic bootstrap. Mol. Biol. Evol. *30*, 1188–1195.
1126 111. Anisimova, M., Gil, M., Dufayard, J.-F., Dessimoz, C., and Gascuel, O. (2011). Survey of
1127 Branch Support Methods Demonstrates Accuracy, Power, and Robustness of Fast
1128 Likelihood-based Approximation Schemes. Syst. Biol. *60*, 685–699.
1129 112. Bininda-Emonds, O.R. (2005). transAlign: using amino acids to facilitate the multiple
1130 alignment of protein-coding DNA sequences. BMC Bioinformatics *6*, 156.
1131 113. Anisimova, M. ed. (2012). Evolutionary Genomics: Statistical and Computational Methods,
1132 Volume 2 (Springer Science+Business Media, LLC).
1133 114. dos Reis, M., and Yang, Z. (2011). Approximate likelihood calculation on a phylogeny for
1134 Bayesian estimation of divergence times. Mol. Biol. Evol. *28*, 2161–2172.
1135 115. Douglas, J., Zhang, R., and Bouckaert, R. (2021). Adaptive dating and fast proposals:
1136 Revisiting the phylogenetic relaxed clock model. PLOS Comput. Biol. *17*, e1008322.
1137 116. Huson, D.H., Klöpper, T., Lockhart, P.J., and Steel, M.A. (2005). Reconstruction of
1138 Reticulate Networks from Gene Trees. In Research in Computational Molecular Biology
1139 Lecture Notes in Computer Science., S. Miyano, J. Mesirov, S. Kasif, S. Istrail, P. A.
1140 Pevzner, and M. Waterman, eds. (Springer), pp. 233–249.
1141 117. Hahn, M.W., and Hibbins, M.S. (2019). A Three-Sample Test for Introgression. Mol. Biol.
1142 Evol. *36*, 2878–2882.
1143 118. Eriksson, A., and Manica, A. (2012). Effect of ancient population structure on the degree of
1144 polymorphism shared between modern human populations and ancient hominins. Proc.
1145 Natl. Acad. Sci. *109*, 13956–13960.
1146 119. Abascal, F., Zardoya, R., and Telford, M.J. (2010). TranslatorX: multiple alignment of
1147 nucleotide sequences guided by amino acid translations. Nucleic Acids Res. *38*, W7–W13.
1148 120. Flouri, T., Jiao, X., Rannala, B., and Yang, Z. (2020). A Bayesian Implementation of the
1149 Multispecies Coalescent Model with Introgression for Phylogenomic Analysis. Mol. Biol.
1150 Evol. *37*, 1211–1223.
1151 121. Hey, J., Chung, Y., Sethuraman, A., Lachance, J., Tishkoff, S., Sousa, V.C., and Wang, Y.
1152 (2018). Phylogeny Estimation by Integration over Isolation with Migration Models. Mol.
1153 Biol. Evol. *35*, 2805–2818.
1154 122. Patterson, N., Moorjani, P., Luo, Y., Mallick, S., Rohland, N., Zhan, Y., Genschoreck, T.,
1155 Webster, T., and Reich, D. (2012). Ancient Admixture in Human History. Genetics *192*,

1065–1093.
123. Huson, D.H., and Bryant, D. (2006). Application of Phylogenetic Networks in Evolutionary Studies. Mol. Biol. Evol. *23*, 254–267.
124. Solís-Lemus, C., Yang, M., and Ané, C. (2016). Inconsistency of Species Tree Methods under Gene Flow. Syst. Biol. *65*, 843–851.
125. Yu, Y., Degnan, J.H., and Nakhleh, L. (2012). The Probability of a Gene Tree Topology within a Phylogenetic Network with Applications to Hybridization Detection. PLOS Genet. *8*, e1002660.